Development of a Scaleable Process for the Synthesis of a Next-Generation Statin

Lindsay A. Hobson,* Otute Akiti, Subodh S. Deshmukh,[†] Shannon Harper, Kishta Katipally, Chiajen J. Lai, Robert C. Livingston,[‡] Ehrlic Lo, Michael M. Miller, Srividya Ramakrishnan, Lifen Shen, Jan Spink,[§] Srinivas Tummala, Chenkou Wei, Kana Yamamoto,[⊥] John Young, and Rodney L. Parsons, Jr.*

Department of Chemical Process Research and Development, Bristol-Myers Squibb Company, One Squibb Drive, New Brunswick, New Jersey 08903, U.S.A.

Abstract:

This manuscript details the process research and development of a convergent and safe approach to 1 on a multikilo scale. Specific highlights of the process development efforts will be described, including the development of a dehydrogenation method for dihydropyrimidines and a thermochemically safe synthesis of a 1,2,4-aminotriazole fragment. A key feature of the synthesis is the use and optimization of a modified Julia−Kocienski olefination reaction. Specifically, we report an unprecedented dependence of the product olefin geometry on reaction temperature, where an *E:Z* ratio as high as 200:1 can be obtained. Initial insights into the mechanistic rationale for this observation are also provided. Finally, a purity upgrade sequence via an intermediate crystalline form is highlighted as a method of controlling the final API quality.

Introduction

Coronary heart disease is a leading cause of death worldwide. The risk of coronary heart disease is increased in individuals having elevated concentrations of plasma low density lipoprotein cholesterol (LDL-C).[1] In the fight against coronary heart disease statins,[2] HMGR inhibitors represent the gold standard in treating hypercholesterolemia and mixed dyslipidemia. Although many marketed statins are effective in lowering levels of LDL-C they have also been linked to a variety of skeletal muscle related problems such as cramping, myalgia,[3] and rhabdomyolysis.[4] The Discovery Chemistry group within Bristol-Myers Squibb focused on identifying a potent and efficacious HMGR inhibitor with a potentially superior safety profile; to that end BMS-
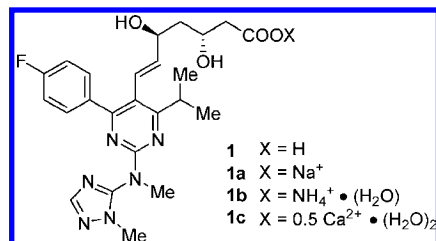

Figure 1. Structure of target compound 1.

644950, **1**, was identified for advancement into clinical development (Figure 1).[5]

Results and Discussion

The starting point for the synthetic route development was the Discovery synthesis outlined in Scheme 1.[5] Their approach involved the preparation of intermediate **6** in a three-step sequence from the previously reported pyrimidine **2**.[6] Diisobutylaluminum hydride reduction of ester **2** followed by TEMPO oxidation afforded the corresponding aldehyde **4** in 60% overall yield. Aldehyde **4** was converted to intermediate **6** via the employment of a Julia−Kocienski olefination[7] using the previously described sulfone **5**.[8] Next, treatment of intermediate **6** with the anion of 1-methyl-1H-1,2,4-triazol-5-amine, **7**, generated via deprotonation with lithium hexamethyldisilazide in THF/DMF, afforded intermediate **8a** which on exposure to methyl iodide provided intermediate **8b**. Subsequent deprotection of the acetonide with HCl and removal of the *tert*-butyl group with sodium hydroxide afforded **1a** as the sodium salt. While this sequence met the Discovery material requirements and was amenable to preparing analogues of **6**, consideration from the process perspective revealed a number of synthetic challenges.

First, the synthesis was a long linear sequence requiring the extensive use of column chromatography, primarily for impurity

* To whom correspondence should be addressed. E-mail: lindsay.hobson@bms.com; rodney.parsons@bms.com.

† Current address: Chemical and Pharmaceutical Development, Wyeth Research, Pearl River, NY 10965.

‡ Current address: Process Development, Gilead Sciences, Inc., 333 Lakeside Drive, Foster City, CA 94404.

§ Current address: Johnson & Johnson, PRD, L.L.C., Welsh and McKean Roads, P.O. Box 776, Spring House, PA 19477-0776.

⊥ Current address: Department of Chemistry, University of Toledo, 2801 W. Bancroft St., Toledo, OH 43606.

(1) Third Report of the National Cholesterol Education Program (NCEP) Expert Panel on Detection, Evaluation, and Treatment of High Blood Cholesterol in Adults (Adult Treatment Panel III) final report. *Circulation* **2002,** *106,* 3143−421.

(2) Grundy, S. M. *J. Intern. Med.* **1997,** *241,* 295–306. Ross, S. D.; Allen, I. E.; Connelly, J. E.; Korenblat, B. M.; Smith, M. E.; Bishop, D.; Luo, D. Clinical Outcomes in statin treatment trials: a meta-analysis. *Arch. Intern. Med.* **1999,** *159,* 1793–1802.

(3) For a review, see: Rosenson, R. *Am. J. Med.* **2004,** *116,* 408–416.

(4) Graham, D. J.; Staffa, J. A.; Shatin, D.; Rade, S. E.; Schech, S. D.; La Grenade, L.; Gurwitz, J. H.; Chan, K. A.; Goodman, M. J.; Platt, R. *JAMA, J. Am. Med. Assoc.* **2004,** *292,* 2585–2590.

(5) Ahmad, S.; Madsen, C. S.; Stein, P. D.; Janovitz, E.; Huang, C.; Ngu, K.; Bisaha, S.; Kennedy, L. J.; Chen, B.-C.; Zhao, R.; Sitkoff, D.; Monshizadegan, H.; Yin, X.; Ryan, C. S.; Zhang, R.; Giancarli, M.; Bird, E.; Chang, M.; Chen, X.; Setters, R.; Search, D.; Zhuang, S.; Nguyen-Tran, V.; Cuff, C. A.; Harrity, T.; Darienzo, C. J.; Li, T.; Reeves, R. A.; Blanar, M. A.; Barrish, J. C.; Zahler, R.; Robl, J. A. *J. Med. Chem.* **2008,** *51,* 2722–2733.

(6) Watanabe, M.; Koike, H.; Ishiba, T.; Okada, T.; Seo, S.; Hirai, K. *Bioorg. Med. Chem.* **1997,** *5,* 437–444.

(7) Blakemore, P. R.; Cole, W. J.; Kocienski, P. J.; Morley, A. *Synlett* **1998,** *1,* 26–28. Baudin, J. B.; Hareau, G.; Julia, S. A. *Tetrahedron Lett.* **1991,** *32,* 1175. For recent reviews, see: Plesniak, K.; Zarecki, A.; Wicha, J. *Top. Curr. Chem.* **2007,** *275,* 163–250. Blakemore, P. R. *J. Chem. Soc., Perkin Trans. 1* **2002,** 2563–2585.

(8) Brodfuehrer, P. R.; Sattelberg, T. R., Sr.; Kant, J.; Qian, X. Process for preparing chiral diol sulfones and dihydroxy acid HMG-CoA reductase inhibitors. PCT Int. Appl. WO/2002/098854.

Scheme 1. Discovery chemistry route designed for SAR exploration
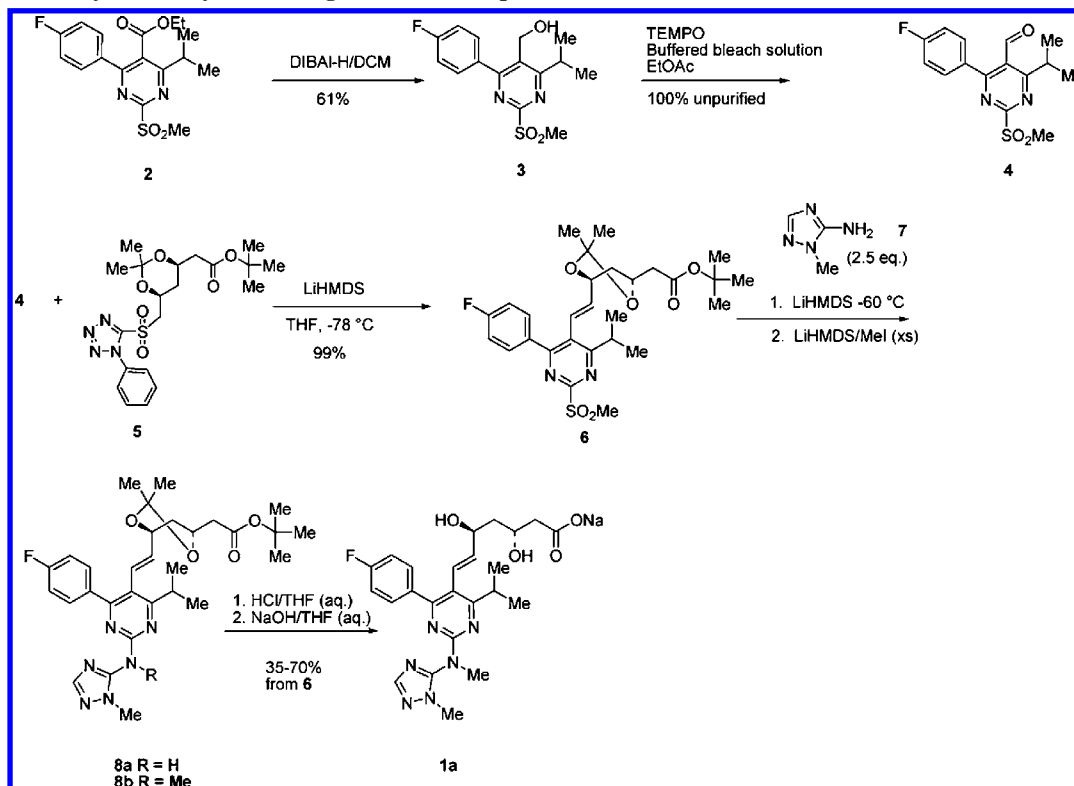
removal and also some of the intermediates were found to be noncrystalline. A primary goal would be to eliminate the requirement for chromatographic purification in order to maximize the throughput of the sequence. The achievement of this goal would be realized through the identification of crystalline intermediates throughout the sequence that could serve as control points for purity. Second, control of the stereochemical integrity would be of significant concern during the synthesis due to the acid lability of the acetonide and the susceptibility of the C-5 hydroxyl to undergo epimerization. Control would also be needed in the preparation of the *trans*-olefin geometry. The synthesis utilized by the Discovery Chemistry group to prepare aminotriazole, **7**, generated methanethiol, a highly flammable and toxic gas which would present safety concerns for pilot scale manufacture therefore an alternative synthesis of **7** would be required for multikilogram-scale production.

Toward this end retrosynthetic analysis of **1** suggests the late-stage installation of the olefin via sulfone **5**, preceded by disconnection to aminotriazole **7** leading to the known pyrmidine core **10**, Scheme 2.[9] Strategically, forming the trans-olefin using a modified Julia−Kocienski olefination[7] would provide a complementary method to other olefination methods previously utilized on these types of substrates,[9] as well as utilizing established technology from within our department.[8] Introduction of chirality through sulfone **5** at the penultimate step of the synthesis would minimize the potential for epimerization at the C-5 hydroxyl position as well as allow for a simple transformation at the final step, removal of the acetonide and

tert-butyl groups. Sulfone **5** can be prepared from a known procedure in three steps from the commercially available Kaneka alcohol as outlined by Brodfuehrer et al.[8] The synthesis of pyrimidine core **10** could be readily achieved in three steps from the commercially available 4-fluorobenzaldehyde, urea, and isobutyryl acetate, through a sequence utilized to prepare a key intermediate in the rosuvastatin synthesis.[10]

Synthesis of Chloropyrimidine, 10. Utilizing a previously described procedure chloropyrimidine **10** could be prepared through a three-component Biginelli coupling reaction,[11] followed by oxidation and electrophilic activation, Scheme 3.[10]

The Biginelli three-component coupling reaction effectively provides pyrimidinone **11** after refluxing the three reagents in methanol with catalytic copper(I) chloride and sulfuric acid for 24 h. The product crystallized directly from the reaction mixture; however, during development of the process an exotherm was observed upon crystallization. To circumvent this exotherm, on-scale seeding was employed prior to the onset of crystallization. Conversion of **11** into **12** required an oxidation, which in the literature had been performed by adding compound **11** directly into a solution of 65% nitric acid.[10] In developing this process we were cognizant of potential safety risks that could occur from this reaction, and we sought to investigate the thermochemical aspects of the process. Upon evaluation of the safety of the reaction it was found that the oxidation chemistry exhibited the potential for a temperature-dependent uncontrollable runaway as outlined in the graphs in Figure 2.

The graph in Figure 2a shows the kinetic safety profile, specifically the time−temperature relationship for a thermo-

(9) Koike, H.; Kabaki, M.; Taylor, N. P. Process for the production of *tert*-butyl (*E*)-(6-[2-[4-(4-fluorophenyl)-6-isopropyl-2-[methyl(methylsulfonyl)amino]pyrimidin-5-yl]vinyl]-(4*R*,6*S*)-2,2-dimethyl[1,3-dioxan-4yl)acetate. PCT Int. Appl. WO/2000/49014, 2000.
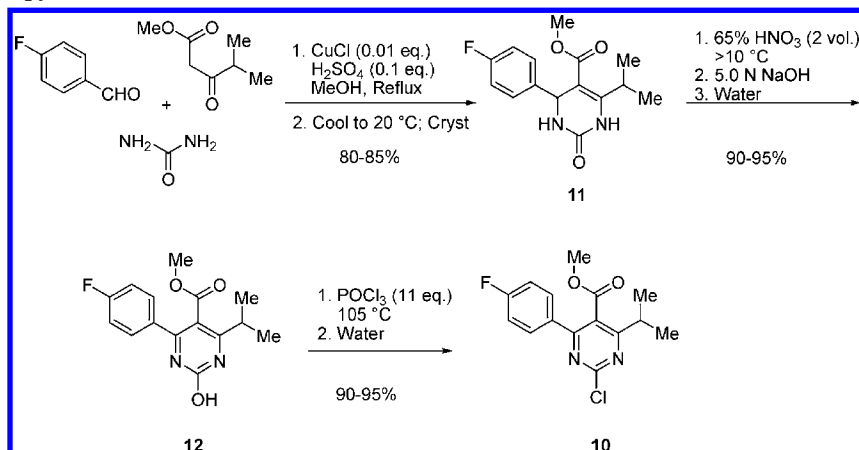
(10) Matsushita, A.; Oda, M.; Kawachi, Y.; Chika, J. Preparation of aminopyrimidine compounds. PCT Int. Appl. WO/2003/006439 A1, 2003.

(11) Biginelli, P. *Gazz. Chim. Ital.* **1893**, *23*, 360–413.

Scheme 2. Structural challenges and retrosynthetic analysis of 1
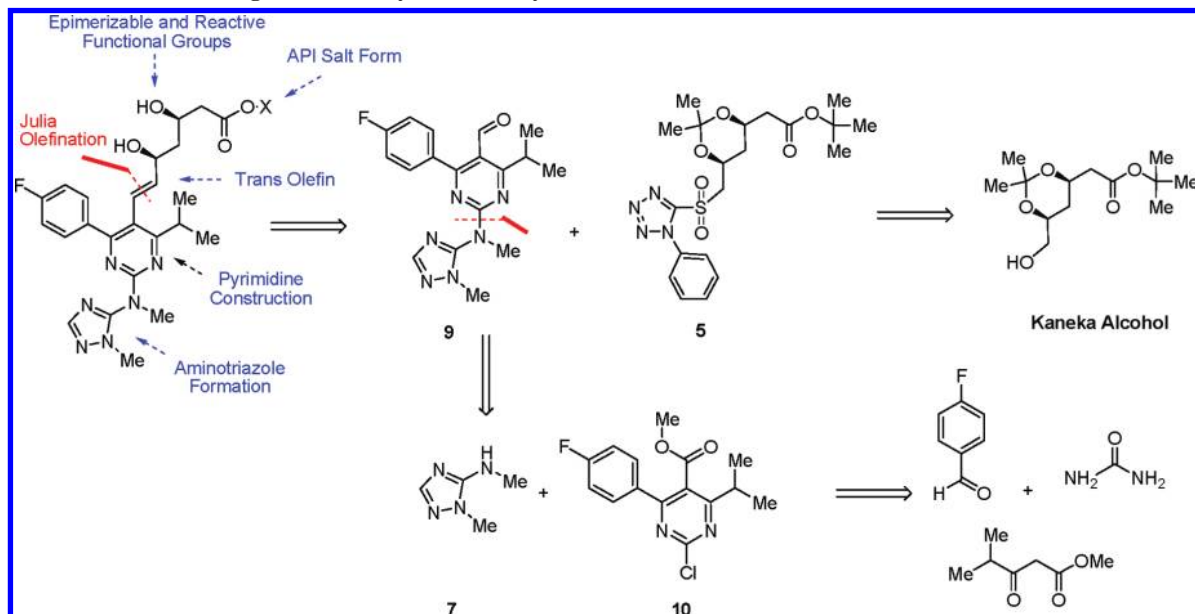
Scheme 3. Synthesis of pyrimidine 10

chemical event. From this plot it can be determined how long the reaction can be held without cooling before it becomes an uncontrollable event. What is most concerning from Figure 2a is the slope of the plot versus the logarithmic scale for time since this indicates that if cooling were to be lost on the reactor then the mixture would self-heat and produce an adiabatic temperature rise of 197 °C, which is the experimental adiabatic temperature rise (125 °C) corrected by the Phi factor (1.58).[12] If this reaction were to reach >40 °C, then it would become unstoppable until all the reagents are consumed as shown by
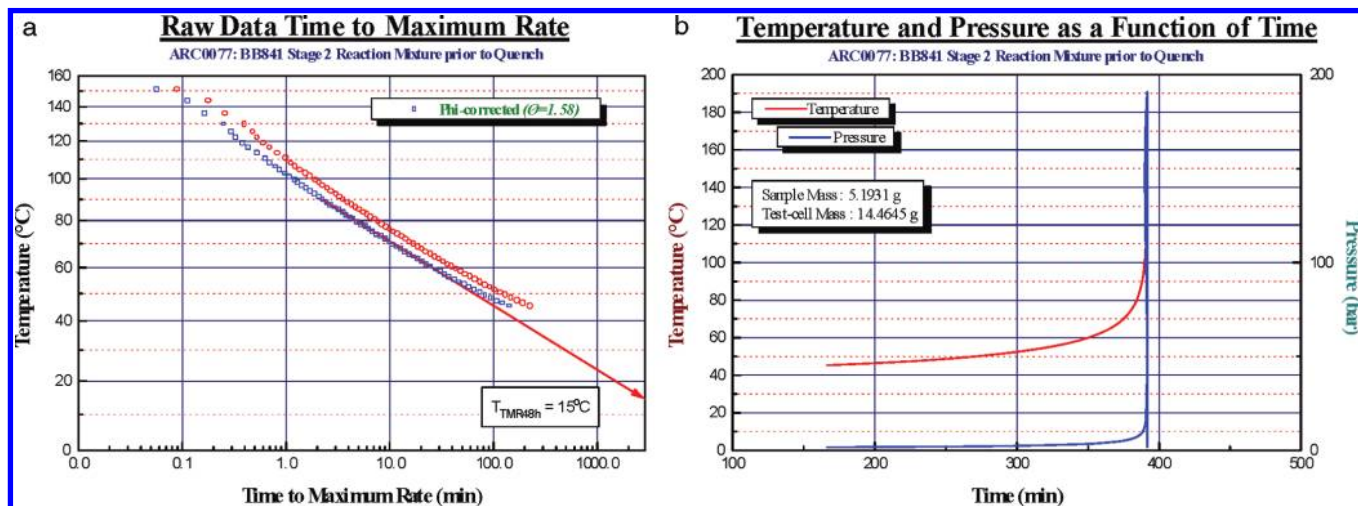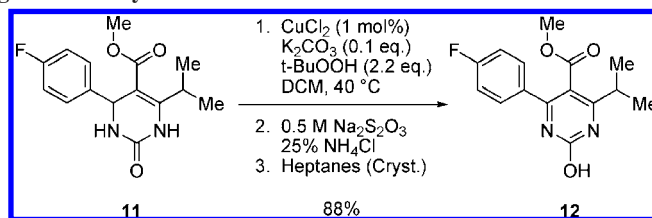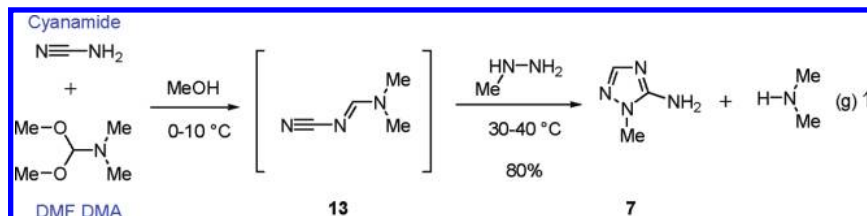

Figure 2. Safety evaluation of the oxidation - ARC results.

Scheme 4. Synthesis of **12** using metal-catalyzed conditions

Scheme 5. Synthesis of aminotriazole **7**

the graph in Figure 2b. Recall that the procedure was to add **11** to the nitric acid, so that, if active cooling was lost and the reaction reached >40 °C, there would be no controls in place to stop the reaction. As a result, the nitric acid oxidation was not viewed as a viable, safe process for scale up, and thus we sought to identify alternative conditions for scale up. To achieve that goal many established oxidation protocols were attempted but were found to be ineffective. For example, the use of DDQ, CAN, or MnO_2 required the use of stoichiometry-based metal reagents and would not be ideal for use on scale. There were also issues encountered with the isolation of the product with respect to removal of the oxidant byproduct. The use of reagents such as Pd/C, $Mn(OAc)_3$, or $NaBrO_3$ led to low-yielding reactions with benzylic oxidation of the side-chain as a major byproduct. After reviewing the literature we turned our attention to investigating metal-catalyzed conditions which had been outlined in a Japanese patent and had been employed on a related series of substrates.[13] The protocol involved the use of a metal catalyst (copper, in particular) together with an oxygen-based oxidant. Evaluation of these copper-catalyzed conditions led to the identification of *tert*-butylhydroperoxide as the preferred stoichiometric oxidant for the reaction, Scheme 4. Furthermore, it was found that a base was an essential additive for the reaction.[14] Following a safety evaluation of the copper-catalyzed conditions we were gratified to find that they were much safer than the nitric acid conditions, since the self-heating event did not occur until 170 °C. This procedure consistently provided **12** in >85% yield and with >99 area % and >97 wt %.

Having addressed the thermochemical issues associated with the oxidation and developed an alternative robust, scaleable process, the next step was to perform electrophilic activation of the pyrimidine ring. This could be readily achieved through treatment of **12** with neat phosphorus oxychloride following the literature procedure to provide **10**.[10] Through incremental modifications, mechanistic understanding, and development of the dehydrogenation method we were able to synthesize >400 kg of **10** in 70−75% overall yield to enable development of the subsequent steps.

Synthesis of Aminotriazole 7. The method utilized by the Discovery Chemistry group to prepare aminotriazole **7** used a procedure reported by Kroger in 1964 which involved the nucleophilic displacement of methanethiol from *S*-methyl-isothiourea sulfate with methylhydrazine followed by treatment of the intermediate guanidine with formic acid.[15] From the process perspective there were a number of concerns identified with this sequence which precluded it from further scale up, primarily the evolution of the highly toxic and flammable methanethiol byproduct together with the need for chromatographic purification. In reviewing the literature for alternative approaches it was found that many of the known methods for preparing 1,2,4-triazoles would not be applicable for the preparation of the 5-substituted aminotriazole **7**. A report by Selby in 1984 outlined a protocol which used dimethylcyano-carbonimidate and methylhydrazine to prepare 3,5-substituted triazoles, and this ultimately provided the basis for a modified synthesis of **7**.[16] Based on this procedure, a modification of the cyanocarbonimidate would be needed, and this could readily be achieved through the use of dimethylformamide dimethyl-lacetal. It was gratifying to find that reaction of cyanamide with dimethylformamide dimethylacetal in methanol provided uniso-lated intermediate **13**, which on reaction with methylhydrazine at 30−40 °C formed the desired 5-aminosubstituted triazole **7**, in high overall yield, 75−85%, Scheme 5. The process development to enable the successful preparation of 280 kg of **7** in high purity (99.9 area%, 99.4 wt %) will be reported in due course.[17]

There is, however, one disadvantage to this approach in that it does not allow for the simultaneous installation of both of the required methyl groups. To accomplish this in the current synthesis of **7** a modification of cyanamide to incorporate a methyl group on the nitrile nitrogen would be required; unfortunately, this was not feasible. Since the methyl group could not be directly incorporated during the synthesis of the

(12) Data collected in collaboration with SAFC Gillingham, Dorset, United Kingdom.
(13) Metal-catalyzed oxidations in related systems: Kuwabe, T.; Okuyama, S.; Hashimoto, S. Jpn. Kokai Tokkyo Koho; JP 10114755 A2 19980506 Heisei, 1998.
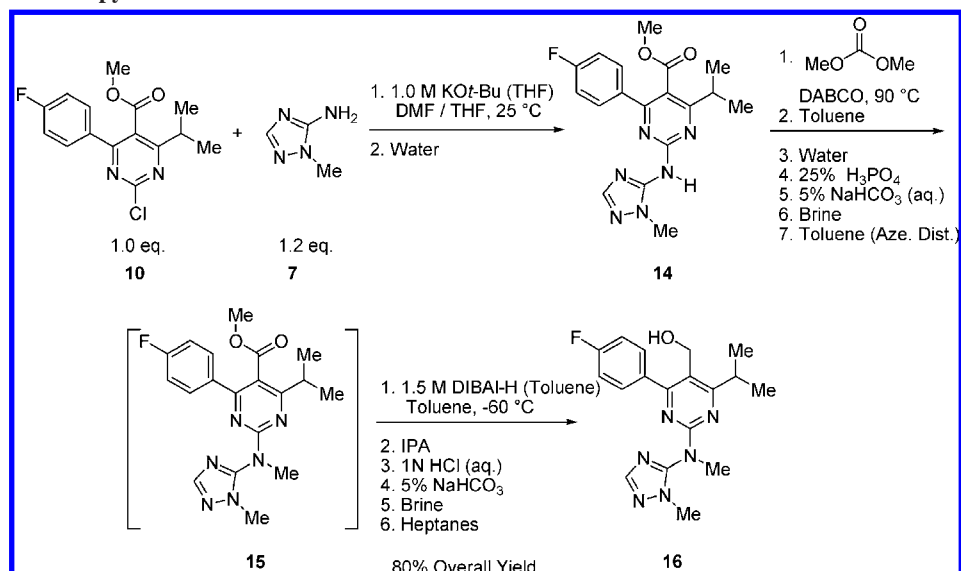(14) For scope and details of the mechanistic study performed on this reaction see: Yamamoto, K.; Chen, Y. G.; Buono, F. G. *Org. Lett.* **2005**, *7*, 4673–4676.
(15) Kroger, C.; Schoknecht, G.; Beyer, H. *Chem. Ber.* **1964**, *97* (2), 396–404.
(16) Selby, T. P.; Lepone, G. E. *J. Heterocycl. Chem.* **1984**, *21*, 61.
(17) Katipally, K. *Synth. Commun.* Manuscript in progress.

Scheme 6. Completion of pyrimidine core **18**

triazole core, attempts were made to methylate compound **7**. Various bases and methylating reagents were screened but with limited success due to difficulties in separating the desired compound from a mixture of regioisomers and dimethylated products. The most promising approach was through a reductive amination with formaldehyde; however, this met with challenges ranging from a mixture of products, low yields, and difficulties in isolating clean product. As a result of these challenges together with the time constraints in which this fragment was needed it was decided to investigate the installation of the methyl group at a later stage in the synthesis.

Completion of Pyrimidine Core 18. With a robust, scaleable synthesis capable of producing multikilo quantities of **7** the next step required coupling to chloropyrimidine **10**. From the literature it was known that nucleophiles such as *N*-methylsulfonamide can displace the chloride;[10] however, the key question for this synthesis to be viable was whether the coupling could be accomplished with a compound such as **7** which bears a poorly nucleophilic amino function.

To effect the coupling of **10** with **7**, various bases such as sodium or potassium hexamethyldisilazide and sodium or potassium *tert*-butoxide were tried. Of these bases sodium or potassium *tert*-butoxide in THF was found to be the most effective for the coupling although some issues were identified with this reaction. First, the reactions performed in THF were heterogeneous due to insolubility of aminotriazole **7**. Second, an impurity derived from the displacement of the chloride with *tert*-butoxide was generated in significant amounts, 2−8 area % in-process, and third, these conditions required an extensive, volume-inefficient extractive workup followed by crystallization to isolate the product. To address these issues and streamline the process alternative reaction conditions were screened including solvent selection and concentration, and this led to the identification of DMF as an essential cosolvent. The addition of DMF led to the solubilization of aminotriazole **7** and also suppressed impurity formation, presumably due to the more facile deprotonation of aminotriazole **7** in solution compared to the heterogeneous mixture. Moreover, following reaction completion product **14** could be directly crystallized from the

reaction mixture by the addition of water, thus eliminating the need for an extractive workup. The product was isolated in 85% yield with typical purities of 99.9 area %, and 99.4 wt % on a 260 kg scale. The next step required methylation of the secondary amine. Having described earlier the previous attempts to methylate aminotriazole **7** with limited success we were pleased to find a procedure developed by Shieh[18] for the N-methylation of indoles using dimethylcarbonate as reagent with catalytic DABCO at 90 °C, Scheme 6. On testing these conditions with substrate **14** we obtained successful methylation; however, due to the long reaction time needed to reach completion several impurities formed which were difficult to purge during the isolation. Simply increasing the amount of DABCO to a stoichiometric charge significantly shortened the reaction time and minimized the impurity formation, whilst successfully achieving methylation to provide compound **15**. The next challenge was in the isolation of **15**; after extensive solvent screening it was found that **15** could not be rendered crystalline, and therefore, the crude product would need to be taken directly into the ester reduction step.

To this end, a telescoped procedure was developed which involved the addition of toluene to the methylation reaction mixture. Following an aqueous workup the toluene solution was dried via azeotropic distillation prior to reduction of the ester group. Attempts to reduce ester **15** directly to aldehyde **9** were met with little to no success, and therefore, it was necessary to reduce ester **15** to alcohol **16** and then reoxidize. To accomplish this, the previously dried toluene solution of **15** was treated with di-isobutylaluminum hydride (1.5 M in toluene) at −60 °C to effect the complete reduction to alcohol **16**. Upon reaction completion the excess hydride was quenched with IPA and the reaction mixture neutralized by inverse addition into HCl. After an aqueous workup the product was crystallized from *n*-heptane/toluene. During the crystallization of **16** it was found that the compound had a tendency to entrain toluene which proved difficult to remove during drying. To displace toluene from the wet cake a heptane wash was incorporated into the filtration

(18) Shieh, W.-C.; Dell, S.; Bach, A.; Repic, O.; Blacklock, T. *J. Org. Chem.* **2003**, *68*, 1954–1957.

Scheme 7. Impurities observed in aldehyde 9
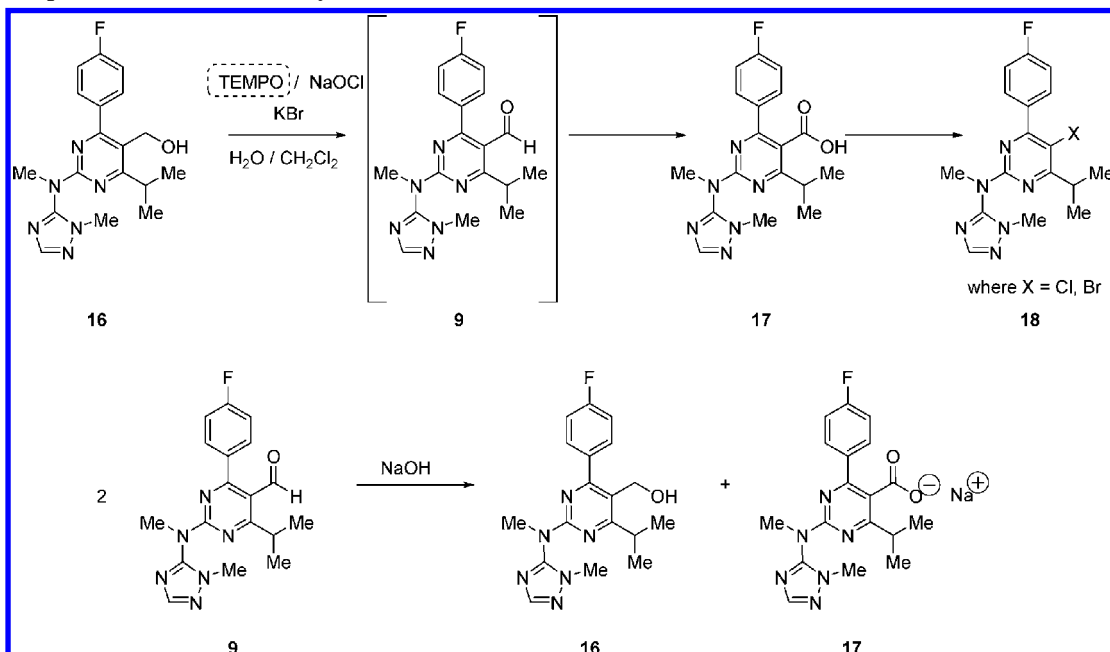
step, and following this **16** was isolated in 80% yield from **10**. During the course of the development activities >500 kg of **16** were produced using the described six-step sequence in 58% overall yield with high quality and purity (>99.4 area % and >98.4 wt %).

Completion of the Synthesis and Formation of 1. With the core of the molecule completed the next step was to perform the oxidation to aldehyde **9**, the precursor needed for the Julia−Kocienski olefination reaction. Taking advantage of internal knowledge it was decided to develop a TEMPO oxidation since this had not only been employed by the Discovery Chemistry team but had also been used within the process group at scale for a similar compound. During early development efforts when the typical catalytic system[19] involving TEMPO, KBr as a cocatalyst, aqueous buffered NaOCl, and DCM as solvent was utilized, a number of processing issues were immediately highlighted. These included an unsatisfactory impurity profile, the stability of the NaOCl reagent in the buffered solution, and the need for a more robust workup and isolation protocol.

During the development of this step several impurities were identified, which included the formation of the corresponding acid **17** as a result of overoxidation and generation of halide impurities **18** which could potentially form from a decarboxylation pathway of the acid, Scheme 7.[20] Another side reaction observed during the conversion of **16** to **9**, was a base-catalyzed disproportionation of two aromatic product aldehydes **9** into the corresponding alcohol **16** and acid **17**. This Cannizzaro reaction[21] accounts for the instances where small amounts of alcohol **16** are observed in the isolated solid, though not in the in-process control sample. Screening reaction conditions using DOE led to an optimized reaction stoichiometry (0.1 equiv of TEMPO, 0.05 equiv of KBr, 1.12 equiv of NaOCl) which

minimized the formation of these side products. In addition, process controls were implemented for NaOCl concentration prior to charging, reaction conversion, and also for acid impurity **17** during the workup.

Typically the TEMPO reaction is buffer dependent due to the equilibrium composition of aqueous solutions of NaOCl. When the bleach (Clorox) or the reaction mixture is buffered (pH 8.5 to 9.5), HOCl is the co-oxidant and is believed to be distributed between the biphasic reaction mixture. In the presence of KBr, HOCl is likely converted to HOBr, which is thought to more efficiently oxidize TEMPO to the oxoammonium ion. One issue observed with buffering the bleach was that the potency decreased by nearly 50% over a 12 h time frame. It is also known that higher concentrations of NaOCl can decrease in potency by 20% per month during storage,[22] thus making a titration of the NaOCl essential when needing to limit overoxidation. To eliminate the observed instability of the buffered NaOCl and increase the general robustness of the process, alternative reaction conditions were explored. It was found that, when nonbuffered/nondiluted NaOCl was charged in a portionwise manner, the product formation was controlled on the basis of reagent charge without a latent exothermic event, as shown by the flat heat signature line in Figure 3. In addition, one could track the formation of product (on the basis of HPLC conversion) directly with the theoretical %NaOCl dispensed.

(19) Anelli, P. L.; Biffi, C.; Montanari, F.; Quici, S. *J. Org. Chem.* **1987**, *52*, 2559−2562. Anelli, P. L.; Montanari, F.; Quici, S. *Org. Synth.* **1990**, *69*, 212−219.

(20) Interestingly, removal of 2,2,6,6-tetramethylpiperidin-1-oxyl (TEMPO) from the reaction does not prevent the formation of this impurity. In fact, it seems as though the alcohol, aldehyde, and acid all afford this late-eluting impurity upon treatment with bleach and KBr in CH$_2$Cl$_2$. A mechanistic understanding for these processes is still being developed. It should be noted that, although this putative halide is an impurity in the oxidation of **18**, its overall abundance is significantly low when employing the conditions developed. The crystallization conditions used to isolate **9** have also been shown to purge most, if not all, of this side product.

(21) Cannizzaro, S. *Ann.* **1853**, *88*, 129. List, K.; Limprich, H. *Ann.* **1854**, *90*, 180.

(22) Mohrig, J. R.; Nienhuis, D. M.; Linck, C. F.; Van Zoeren, C.; Fox, B. G.; Mahaffy, P. G. *J. Chem. Educ.* **1985**, *62*, 519−521.
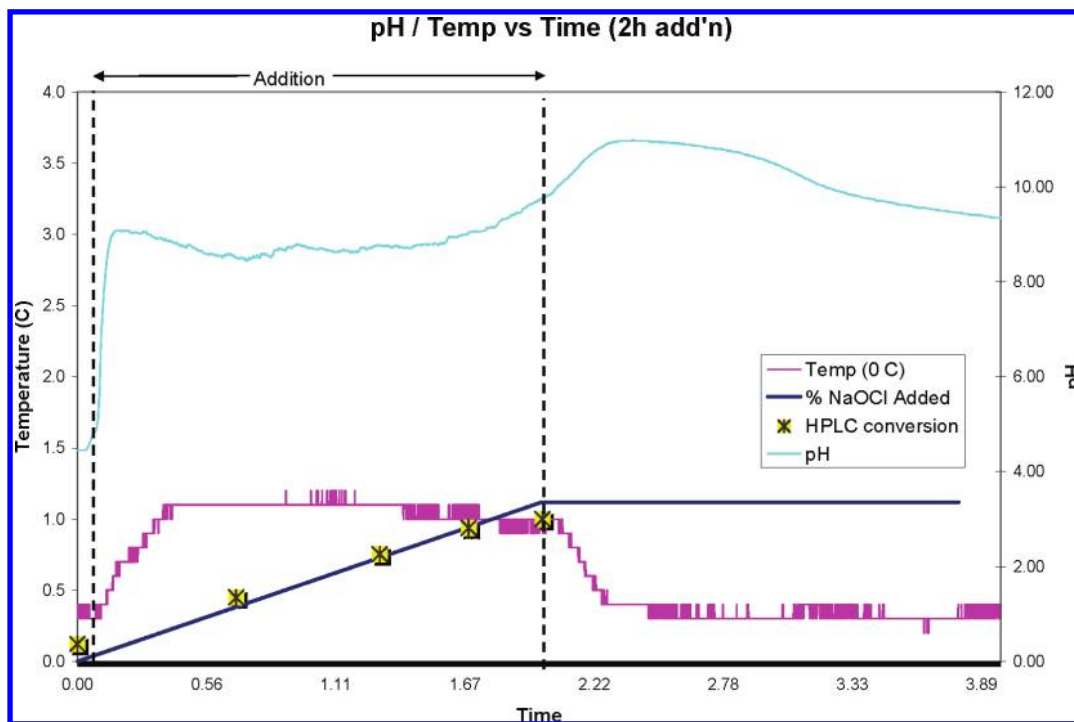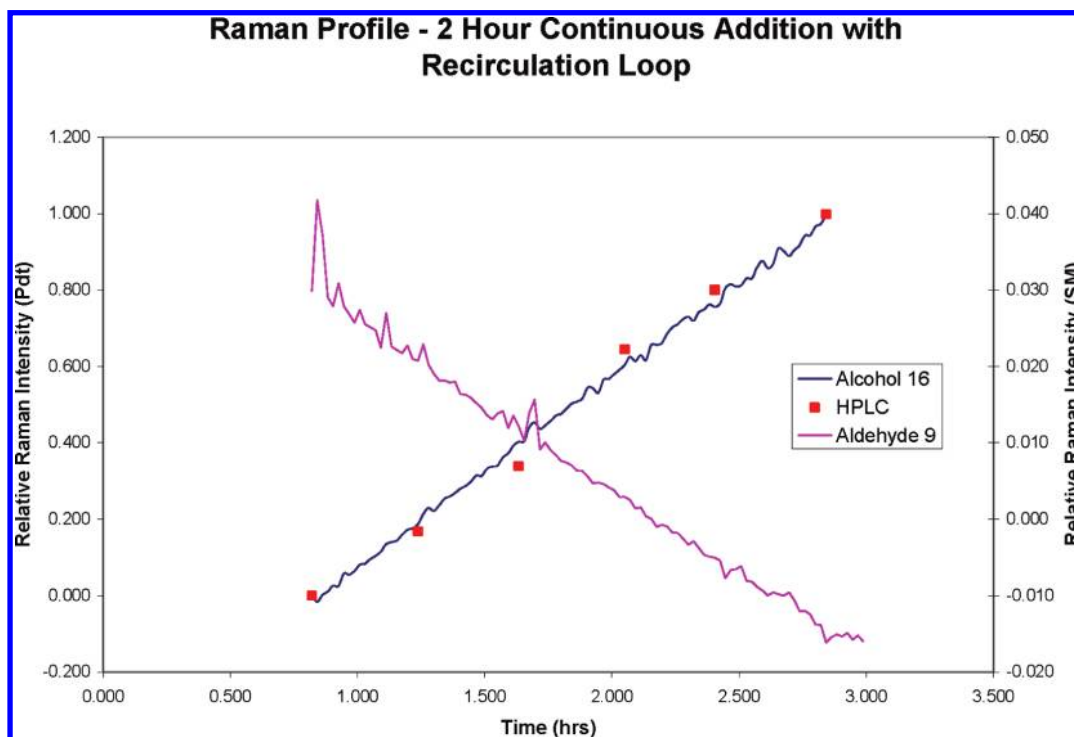
Figure 3. Graph of pH versus addition time.

Figure 4. Raman profile to show conversion of **16** into **9**.

The nonbuffered conditions also led to reduced levels (<0.15 AP) of the overoxidized product, **17**.

In order to minimize sampling, an in-line Raman spectroscopy method was investigated to monitor the oxidation of **16** to **9**. The in-line Raman was able to effectively track both starting material and product during the reaction and the signal correlated well with the HPLC data taken intermittently during the course of the reaction, Figure 4. The Raman could be further used to ensure safe execution as it could detect whether there
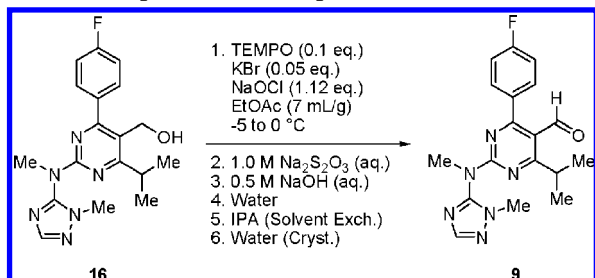
was an induction period during the addition of the NaOCl solution, and it could also be used to avoid reagent accumulation.

The development of a crystallization protocol for **9** employed a standard screen of sixteen (16) solvents with six (6) antisolvents and identified two solvent systems: 1:1 EtOH/H_2O and 1:1 IPA/H_2O. Investigation of the EtOH/H_2O crystallization protocol provided excellent yield and purity; however, needle-like crystals were produced which showed a strong tendency to agglomerate, Figure 5. These agglomerated crystals made
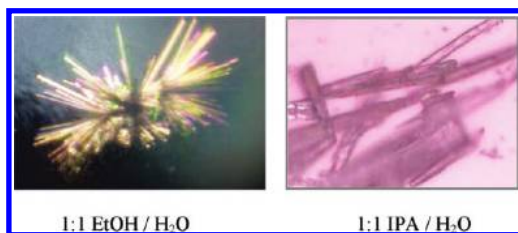
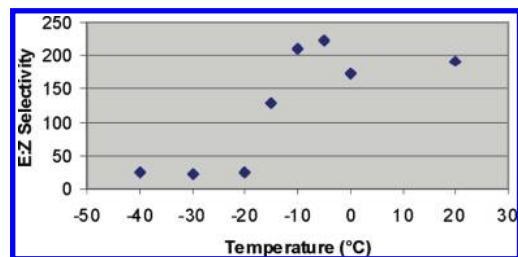**Figure 5.** Comparison of crystals from different solvent systems.

Scheme 8. Improved TEMPO process

Figure 6. Impact of warming on the selectivity and yield of the modified Julia olefination.

filtration and washing operations difficult; therefore, optimization of the IPA/H$_2$O conditions were pursued. The IPA/H$_2$O solvent system provided more granular crystals that did not agglomerate and thus facilitated filtration and drying. An additional benefit of the IPA/water system was that it was superior in purging process impurities to <0.1 area %, while yielding compound **9** in 94% yield with >99.36 wt %.[23]

The oxidation process underwent several process improvements of which the most important from a process perspective was to use nonbuffered NaOCl. As noted earlier this is outside the experiences of what has been generally discussed in the literature and circumvents the reagent instability of buffered NaOCl. The use of Raman analysis in conjunction with HPLC for reaction monitoring was demonstrated during pilot-plant implementation at 30 kg scale to produce **9** in 93.5% yield, 99.88 area %, and 99.63 wt %. Scheme 8.

The final bond-forming reaction in our convergent synthesis was to couple chiral fragment **5** with aldehyde **9** via an appropriate olefination method. To utilize previously developed technology from within our department we focused our efforts on the modified Julia olefination,[7] specifically on phenyltetrazolyl sulfone **5** derived in three steps from the commercially available Kaneka alcohol. While the lithium salt of **5** was found

to be unstable even at cryogenic temperatures, conducting the reaction under Barbier conditions[7] provided satisfactory conversion with only 1.1 equiv of the sulfone required. Procedurally, the reaction was executed by addition of LiHMDS (1 M solution in THF) to a mixture of sulfone **5** and aldehyde **9** in THF below −70 °C, followed by cold quenching with aqueous ammonium chloride, to provide the desired alkene **8** in 85% yield. Under these conditions, the E-olefin was generated with 15:1 selectivity over the Z-isomer, which was effectively purged during the final crystallization of **8b** from ethanol and water. Implementation at the kilogram scale (3 × 3.5 kg of aldehyde **9**) provided olefin **8b** in consistently high yield (85−86%) and quality (99.7−99.8 area %).

Although 15:1 selectivity was sufficient for initial purposes, we sought to improve the performance of the olefination reaction. To accomplish this goal, a number of reaction parameters (temperature, deprotonating base, counterion of base, and reaction solvent) were evaluated to ascertain their influence on the observed E:Z selectivity in our system. On the basis of these studies, temperature was found to have the most significant impact on the observed E:Z ratio. Surprisingly, it was not the temperature at which the initial reaction was performed but rather the temperature post reagent addition (i.e., reaction age temperature) that impacted the observed E:Z ratio. Specifically, our temperature-selectivity dependence studies focused on three specific process phases: the reagent addition temperature, the reaction age temperature, and the quench temperature. When the deprotonating base is added at higher temperatures (>−78 °C) the selectivity for the E-olefin is reduced, and the impurity profile for the reaction is also negatively impacted. To assess the influence of reaction age temperature on selectivity we conducted a series of parameter matrix studies where the age temperature and hold periods were varied. The temperatures evaluated ranged from −70 to 10 °C and hold times from 30 min to 2 h. These studies clearly showed an increase in the observed E:Z ratio when the reaction mixture was aged at noncryogenic temperatures, Figure 6. The reaction age duration also impacted both the observed E:Z ratio and the measured product HPLC solution yield. Specifically, longer hold times (>1 h) led to a significant decay in solution product content and final isolated yield. This degradation process provided a complex mixture of side products, but the primary pathway involved β-elimination of the acetonide. The final optimized process conditions which provided the best balance of E:Z ratio and product yield involved reagent additions at −70 °C, then warming the reaction mixture to −10 °C and aging for 1 h at −10 °C, followed by reaction quench. These conditions afforded an E:Z selectivity of >100:1 in favor of the E-isomer.

(23) In addition to these optimization studies, a great deal of effort was placed on finding a alternative isolation/crystallization possibility in order to avoid the solvent swap from EtOAc to IPA. After a subsequent screen of solvents and anti-solvents, a crystallization mixture of EtOAc/heptane was chosen for further refinement and development. Solubility of **9** was mapped at different temperatures and various solvent compositions, and 3:1 heptane/EtOAc was chosen as a potential crystallization solvent mixture. Although this provided a crystallization directly from the reaction solvent, an easier filtration due to the larger granular crystals generated, and improved drying efficiency, the recovery was plagued with issues during discharge from the reactor (i.e., a semi-stickiness of the resulting solid or possible nucleation/crystallization on the walls of the vessel). Diminished yields (63 M% for 1:1 heptane/EtOAc; 73−79 M% for 3:1 heptane/EtOAc) due to material loss and inherent solubility of **9** were also observed. Further exploration into temperature effects on the crystallization, different ramping protocols, temperature cycling variants, and seeding regimes were found to be successful and to dramatically reduce the amount of fines present in the final solid. These improvements furnished very large granular crystals and an increased yield (**9**: 92 M%, 100 wt%).

Scheme 9. Formation of 8b through a modified Julia olefination
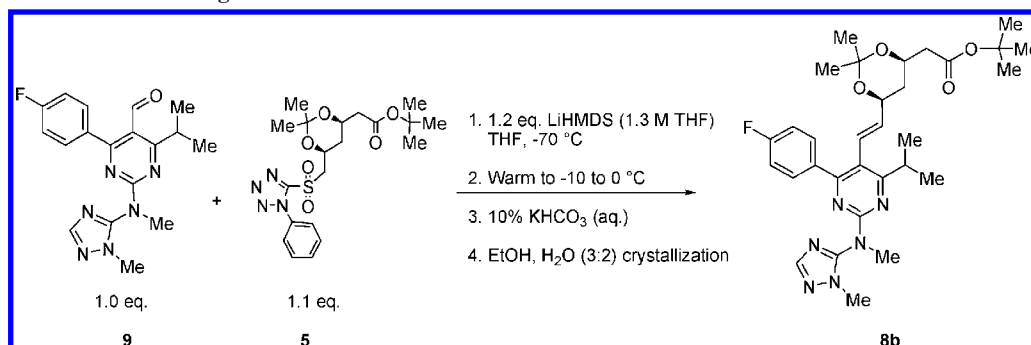
To the best of our knowledge this specific temperature-influencing phenomenon has not been previously reported in the literature. Due to the unexpected nature of these findings and the dramatic enhancement of selectivity, we were prompted to try to elucidate its mechanistic origins. To further evaluate and understand the mechanistic underpinnings and scope of this phenomenon we investigated the reactions with a simplified model system, specifically reactions of benzaldehyde with compound **5**. The parameters studied included the reaction solvent, counterion of the deprotonating base, and reaction temperature. When benzaldehyde was reacted with sulfone **5** (LiHMDS, THF, −78 °C) an E:Z ratio of 60:40 in favor of the Z-isomer was observed when the mixture was aged and quenched at −78 °C. In contrast, warming the reaction mixture to −10 °C and holding for 1 h, resulted in a selectivity reversal and enhancement to afford an 80:20 mixture in favor of the E-isomer. Next, we evaluated the impact of solvent polarity. Aging of the reaction mixtures at noncryogenic temperatures in less polar solvents resulted in an increased E:Z selectivity (solvent selectivity trend was DMF < THF < DME < MTBE < toluene) Changing the counterion of the deprotonating base (Li, Na, K evaluated) also influenced the observed selectivity. Overall, the results indicated that weakly coordinating counterions provide lower E:Z ratios (1.5:1 versus 6:1).

The conclusions from this work are that less polar solvents provide improved E-selectivity under thermodynamic conditions and that the selectivity and isomerization efficiencies are dependent upon the counterion of the base. On the basis of results from the optimization and mechanistic model studies we postulated that the increased selectivity may be due to an equilibration of the initial kinetic intermediate β-alkoxysulfone via a retroaddition/addition pathway. Other mechanistic pathways could be considered, further mechanistic and scope studies are ongoing and will be reported in due course.

Other improvements to the process included replacement of the ammonium chloride quench and sodium bicarbonate wash with two potassium bicarbonate washes. This streamlined processing and was more effective in removing the phenyltetrazolone byproduct, which was not well tolerated in downstream processing. With potassium bicarbonate solutions of sufficiently high ionic strength, it was found that clean phase separations could be achieved without the addition of ethyl acetate as cosolvent to the THF reaction mixture, which improved volume efficiency and greatly shortened the cycle time of the subsequent solvent exchange. The streamlined process was ultimately implemented in the pilot plant (2 × 27 kg of aldehyde **9**) to provide **8b** in 80% average yield with 99.9 area % purity, Scheme 9.

The final stage in the synthesis required the double deprotection of the acetonide and tert-butyl ester groups. The chiral fragment of the molecule was sensitive and susceptible to epimerizations, oxidations, annulations and lactonizations, therefore conditions would not only need to be carefully selected to minimize impurity formation but also the order in which the protecting groups were to be removed would be critical. A key consideration for the deprotection sequence was the identification of a crystalline compound for isolation, since it was known that the free acid was not crystalline. Initial work showed that diol **19** was also not crystalline therefore a suitable salt form would need to be identified. Although the salt would not need to be the final salt form for development, the following attributes would be required: crystalline; robust preparation; and remove process impurities. From the perspective of stability it was found that the acetonide needed to be removed first under acidic conditions, followed by removal of the tert-butyl ester group under basic conditions since this minimized the formation of impurities due to epimerization and lactonization, Scheme 10. Utilization of this strategy would provide a quality control intermediate, which could then be converted into the final pharmaceutically acceptable salt form.

The initial conditions attempted were previously utilized on a similar motif and involved hydrochloric acid (6 N, 3 equiv) in tetrahydrofuran at 20−25 °C to remove the acetonide followed by sodium hydroxide (5 equiv) to remove the tert-butyl group.[24] Employing these conditions with compound **8b** three impurities formed: the epimer at C-5, **20**, and the corresponding lactones **21** and **22** as shown in Figure 7. Using methanol and 2N HCl (2 equiv)[25] at 0−20 °C, provided the intermediate diol ester containing epimer (0.5−1 area %) **20** and a mixture of the tert-butyl ester **19** and methyl ester, both of which could be converted to the carboxylate during the sodium hydroxide step. Reducing the concentration of acid (1 N) provided compound **1** with reduced levels of **20**.[26] Conditions using a catalytic amount of HCl with concentrations of 0.01 N and heating to 40 °C have also been demonstrated on similar compounds.[27] Due to the vast number of combinations for the conditions for the deprotection sequence, it would be difficult to select processing conditions through a typical

---

(24) Private communication with X. Qian.
(25) Private communication with R. Waltermire.
(26) Private communication with S. Ahmad.

Scheme 10. Strategy for removal of the acetonide and *tert*-butyl groups
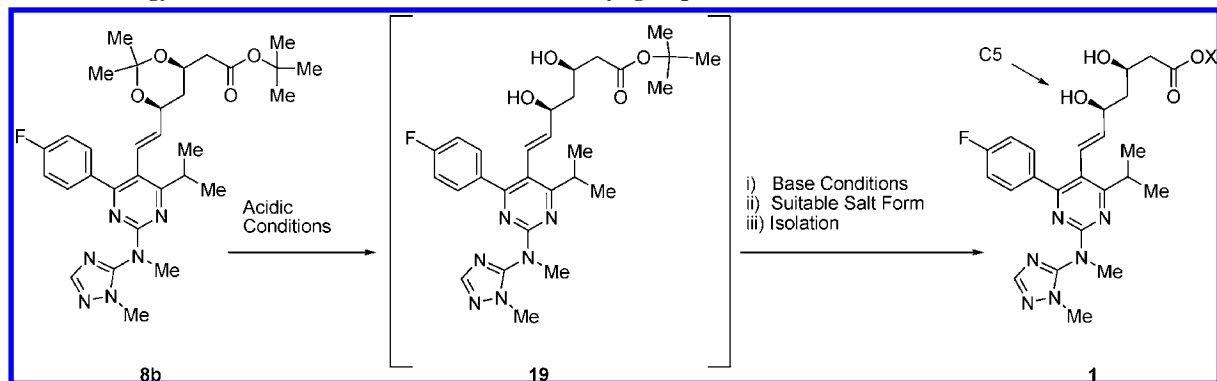
univariate approach. An initial screen of conditions was pursued, followed by a more focused multivariate design of experiments to further define the parameters.
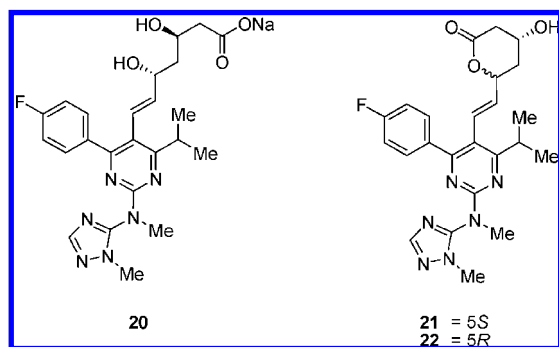
To gain more understanding of the conditions for the deprotection sequence, a screen of different acids (HCl, MSA, sulfuric, acetic, and phosphoric) and solvents (MeCN, THF, acetone, IPA, MeOH, EtOH, DMF, and NMP) was performed. This showed that HCl, sulfuric, and MSA in MeCN or MeOH provided the best results. A larger multivariable screen investigating the design space for the acid equivalents, molarity, temperature, and concentration was then performed, focusing on hydrochloric acid with MeCN and MeOH as outlined in Table 1.

From this study it was found that temperature had the most impact on reaction rate with acid concentration having the next greatest effect. Temperature was shown to impact the degree of epimerization at the C-5 hydroxyl, however this could be minimized through the use of catalytic, dilute acid. Based on these results the deprotection step was further optimized to use a catalytic amount of dilute acid at elevated temperature conditions. The final protocol to remove the acetonide used 0.05 equiv of 0.02 N HCl in acetonitrile (10 vol) at 40−45 °C. After 3 h, <2 area % of **8b** typically remained. Saponification of the *tert*-butyl ester was then readily achieved through the use of

Figure 7. Process impurities observed in the final step.

Table 1. Ranges of conditions tested for the deprotection reaction

| solvent	concentration, mL/g	acid concentration	acid equiv	temp, °C
MeOH[a]	15−30	0.01−0.04	0.02−0.08	35−49
MeCN	7.5−12.5	0.015−0.03	0.03−0.07	35−49

[a] Due to the solubility characteristics of compound **8b** higher volumes of MeOH were needed relative to MeCN.

sodium hydroxide (2 N, 1.5 equiv) at 20−25 °C.[28] These conditions also resulted in the saponification of lactones, **21** and **22**, which formed during the acetonide deprotection. Having developed the deprotection process, all that remained was to identify an acceptable method to isolate the product, *vide infra*, by selection of a suitable salt form of the carboxylic acid. The free acid was a noncrystalline solid which on storage would degrade to epimer **20** and lactones **21** and **22**; the proposed mechanism for decomposition is shown in Scheme 11. Efforts were focused on identifying a salt of **1** since a salt would not be expected to lactonize or epimerize as readily as the free acid.

Initial salt screening focused on pharmaceutically acceptable salts and identified three potential counterions (Na, Ca, and Zn) for development; however, they demonstrated poor crystallization properties, and moreover none of these salts provided any purification upgrade for removing the process-related impurities formed during the deprotection steps. During a screen of amine bases several crystalline leads were identified, methylamine, ammonia, dicyclohexylamine, glycine esters, which were then further investigated for use as an intermediate salt form for purification and isolation. To our surprise the ammonium salt was found to be unusually stable. Single crystal X-ray analysis revealed an array of multiple hydrogen bonds in the crystal structure (which also contained one molecule of water), and the unexpected stability is attributed to this. Ultimately, the ammonium salt was selected as the intermediate salt form to enable isolation from the deprotection sequence due to its ability to purge impurities (Table 2). Only one impurity, **19**, remained at a higher level than the typical qualification threshold, and this was acceptable since it had been qualified in toxicological studies.

The final chemical sequence was then optimized into a telescoped process such that after deprotection of the acetonide and hydrolysis of the *tert*-butyl ester, the pH was adjusted to ∼2 with 1 N hydrochloric acid, and the product was extracted into isopropyl acetate. The isopropyl acetate layer was then water washed and treated directly with either a solution of ammonia in ethanol (2 N) or with ammonia gas. Since the

(27) Taylor, N. P.; Okada, T. Crystalline salts of 7-[4-(4-Fluorophenyl)-6-isopropyl-2-[methyl(methylsulfonyl)amino]pyrimidin-5-yl]-(3R,5S)-3,5-dihydroxyhept-6-enoic acid. (AstraZeneca UK Limited and Shionogi & Co., Ltd.). PCT WO/2001/60804 A1 2001.
(28) The removal of *tert*-butyl esters is typically performed under acidic conditions. The basic conditions had been used previously on a similar compound. Acidic conditions for this molecule would have led to the formation of epimer **20** and lactones **21** and **22**.

Scheme 11. Proposed mechanism for the formation of 20, 21 and 22
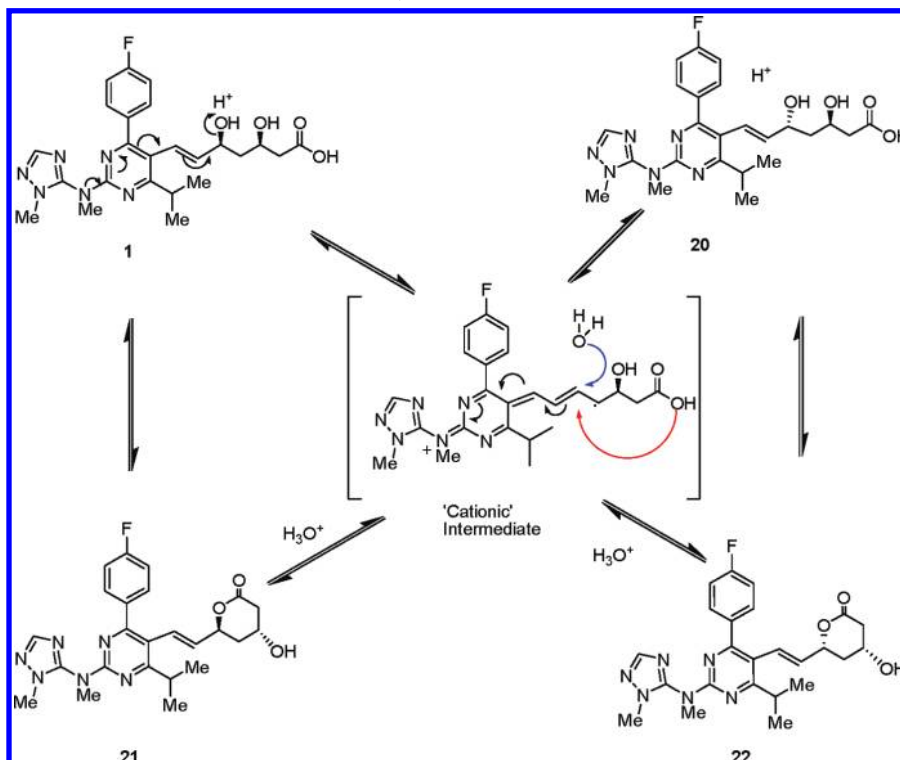
Table 2. Typical purification upgrade during the formation of the ammonium salt with respect to impurities 19−23

| sample	area %[a] 1	area % 19	area % 20	area % 21	area % 22	area % 23
aqueous phase postdeprotection	98.65	0.92	0.19	0.09	<0.03	<0.03
organic phase prior to salt formation	98.44	0.89	0.21	0.09	<0.03	<0.03
dried cake	99.56	0.44	<0.03	<0.03	<0.03	<0.03

[a] Normalized area %.

ammonium salt forms as a monohydrate, it was also essential to have a stoichiometric amount of water present prior to crystallization. By determining the amount of water needed as well as the solubility of water in the organic phase, it was found that additional water charges post aqueous washes were not needed to consistently deliver the salt as its monohydrate. In order to control the nucleation event and crystallization process, seeding with 0.5% of **1b** was implemented. Scheme 12 shows the final sequence from **8b** to **1b**.

Final Form Selection. As noted previously, a significant process challenge for this API was the lack of a suitable crystalline form for development. Despite the beneficial properties of the ammonium salt, (high degree of crystallinity, excellent purity upgrade, reproducible preparation), it was not suitable for use as a final salt form. One major concern was the potential odor due to loss of ammonia in the solid state during long-term storage and further processing. Data from ICH solid-state stability studies performed on ammonium salt **1b** indicated three issues: loss of ammonia when stored in open conditions at elevated temperatures with significant formation of lactone **21**; instability to high-intensity light, with the formation of diastereomeric electrocyclic annulation adducts **23**; and a susceptibility

Scheme 12. Formation of ammonium salt 1b from 8b
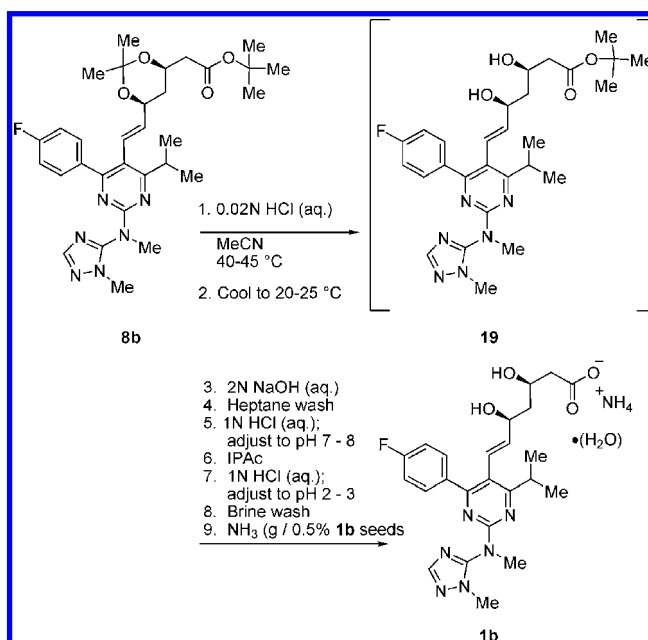
to oxidation when exposed to air with the C-5 hydroxyl being oxidized to form an enone **24**, Figure 8.

In comparison to the ammonium ion, the calcium ion is a pharmaceutically acceptable counterion, and the calcium salt **1c** exhibited acceptable solid-state chemical stability with no lactone formation observed in samples stored at elevated temperatures and humidity, see Table 3. The calcium salt was selected as the final salt form for oral solid dosage development, and this selection was further supported by the prevalence of other marketed statin drugs as calcium salts (e.g., Atorvastatin and Rosuvastatin).[29,30]
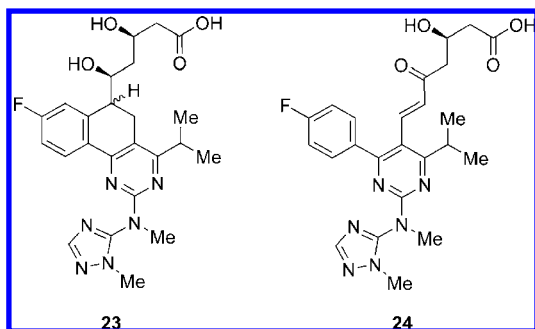
Figure 8. Degradation products observed on stability.

Table 3. Solid state stability of 1c and 1b at specified storage conditions

| storage condition	1c amount remaining area %		1b amount remaining area %	
	1 week	3 weeks	1 week	3 weeks
50 °C (closed)	98.1	98.2	98.6	98.0
40 °C/75% RH (open)	98.6	98.6	96.7	85.0

The calcium salt **1c** did, however, present challenges with regard to its characteristics and preparation. Water was an essential component of the crystal lattice; however, the isolated crystals were found to lose water readily, resulting in an amorphous phase. Overall, the calcium salt was characterized as a weak hydrate with the differential scanning calorimetry (DSC) trace showing a broad endotherm at ∼85 °C due to dehydration and a weak endotherm at ∼130 °C due to melting of the crystals (confirmed by hot stage microscopy), Figure 9. Thermal gravimetric analysis (TGA) of **1c** shows a weight loss between 50 and 110 °C which was attributed to dehydration of the hydrate form, Figure 9. The weight loss of different batches was shown to be variable, depending on the drying conditions used in the preparation. Under controlled drying conditions material having a weight loss between 4 and 7% could be consistently obtained.

Upon examination of the pXRD patterns of various batches of the slurry, wet cake, and dried solids it was found that the patterns varied, depending upon the degree of hydration, Figure 10a. These discrepancies could be attributed to either the existence of a different phase in the slurry or a different hydration state in the solid. Of the calcium salt batches prepared a reproducible pXRD pattern was obtained, although there

appeared to be a degree of amorphous content as indicated by the halo and broad peak shape in the pXRD pattern, Figure 10b. It is important to note that the slurry pattern can be obtained reproducibly when dried powder is reslurried in water; therefore, the hydration/dehydration of the crystals appears to be a dynamic process.

Further evidence for **1c** exhibiting dynamic hydration was obtained from dynamic vapor sorption studies indicating that **1c** was hygroscopic as shown by the gradual weight gain with increasing relative humidity, Figure 11. The lack of a step-isotherm in both adsorption and desorption curves can be indicative of a loose water channel structure for the solid or due to amorphous content in the solid.

From a processing perspective the calcium salt presented significant challenges to the development of a reproducible process for scale up. Two possible approaches were identified for the preparation of **1c**. The first approach involved preparing the free acid from **1b** followed by treatment with a source of calcium ions, and the second approach involved a direct salt exchange from the ammonium to the calcium salt. Upon evaluation of the first approach two issues were immediately identified which precluded further development: the formation of an unstirrable, amorphous gum phase and the instability of the free acid with respect to degradation and impurity formation as discussed earlier. Since this approach was not viable, we turned our attention to the second approach of the direct salt exchange process, Scheme 13. After determining the aqueous solubilities of the ammonium and calcium salts it was found that there was a 2-fold difference in their solubilities which would be advantageous for using an aqueous system for the preparation of **1c**. Ammonium salt **1b** was dissolved in water (20 vol) at 50 °C and treated with a source of calcium ions. Various calcium ion sources such as calcium hydroxide, calcium chloride, and calcium acetate were evaluated, and all provided conversion to the calcium salt. Calcium chloride was selected since it could be added as an aqueous solution. During the early stages of the calcium ion addition, an amorphous gum phase formed which eventually converted to a crystalline material. After exploration of a variety of different addition methods, (calcium ion source added to **1b** or vice versa), it was found that no method was devoid of gum formation. Although this approach appeared straightforward, in practice there were
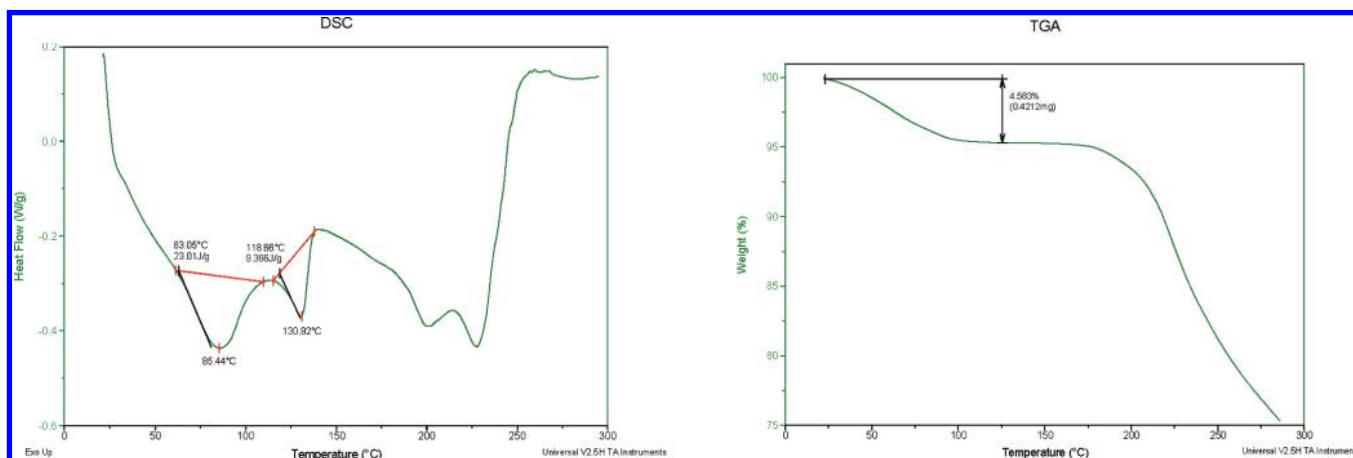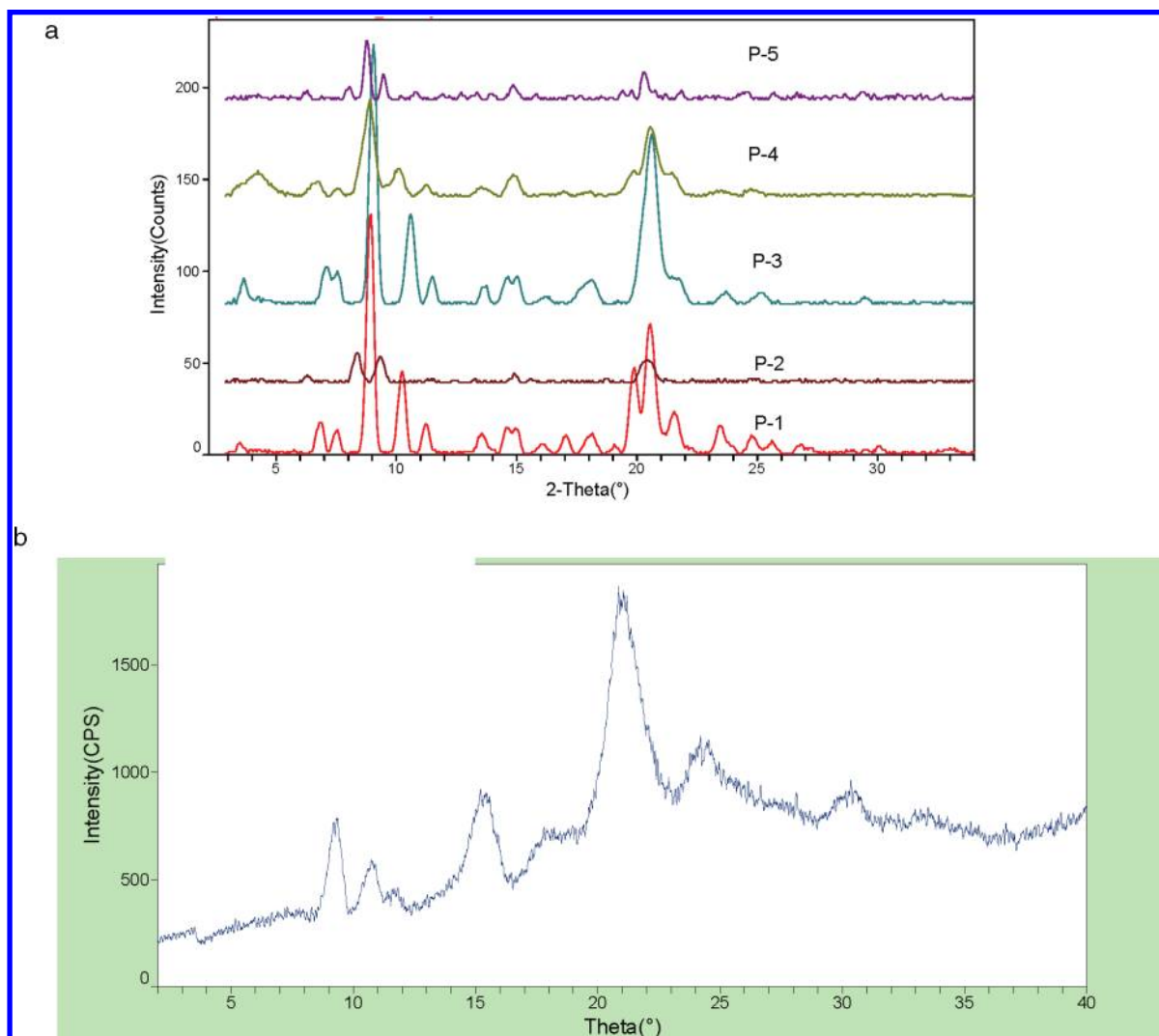

Figure 9. Typical DSC and TGA thermograms of 1c.

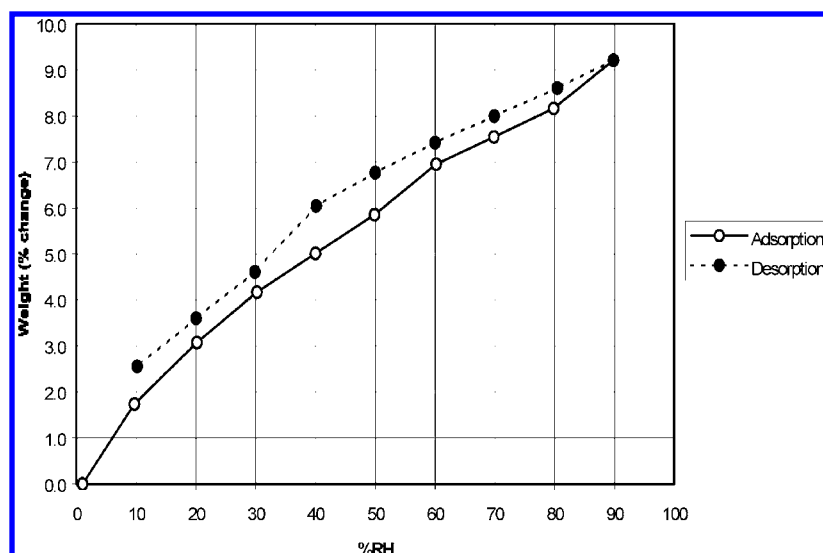**Figure 10.** PXRD patterns of 1c Figure 10b PXRD pattern of 1c dried solid.


Figure 11. Adsorption/desorption curves of 1c.

several aspects which hampered its further development: (1) the high volume of water required for dissolution of **1b** negatively impacted the yield of the reaction, 76% due to the aqueous solubility of calcium salt **1c**; (2) dissolution of **1b** at 50 °C resulted in impurities **20**, **21**, and **22**; and (3) the formation of an amorphous gum phase even when a large excess of seeds were used. The formation of the gum phase is due to product precipitation as a result of the steep solubility profile of the calcium salt in this aqueous system. Furthermore, the crystallization demonstrated slow nucleation kinetics and crystal

Scheme 13. Preparation of **1c** from **1b**
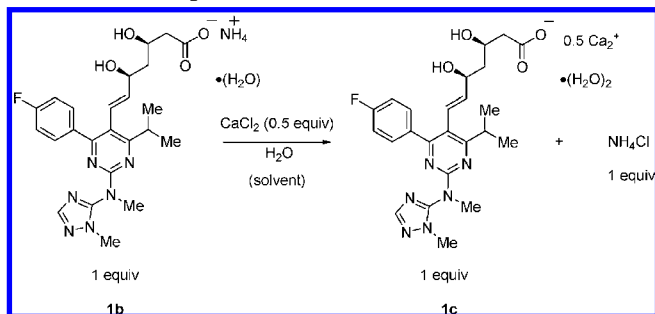
growth rate. The crystal morphology further exacerbated the situation due to being a thin, short needle shape which demonstrated poor filtration rate properties at scale.

In an attempt to address these issues, modifications of this procedure were investigated. A cubic addition profile was employed for the charge of the aqueous $CaCl_2$ solution in an attempt to relieve the rapid supersaturation buildup that plagued linear addition protocols. A cooling step from 52 to 40 °C over 1 h was added after 30% of the $CaCl_2$ charge, in order to establish a seed bed prior to completing the $CaCl_2$ addition. Several temperature cycles between 20 and 50 °C (2 h heating, 15 h aging at 50 °C, followed by a 2 h cooling to 20 °C) were also added to the process in an attempt to increase the particle size by removing fines and thus facilitating filtration.

Although these modifications eliminated the formation of the gum phase through a specific $CaCl_2$ addition and seeding protocol, amorphous material was still evident during the initial stage of the process, and the crystal morphology was still thin, short needles. Also, the yield for these protocols was only 60−65%, due to a significant amount of material lost to the mother liquor and washes due to the relatively high solubility of **1c** in water (10.6 mg/mL). Due to the limitations of these protocols we focused the development efforts on a heterogeneous transformation versus the traditional direct crystallization. During the development of the heterogeneous protocol it was found that the presence of excess $CaCl_2$ dramatically reduced the aqueous solubility of **1c**. A 5−6-fold solubility reduction of **1c** (10.6 mg/mL in pure water versus 2 mg/mL in 3−5 wt % aqueous $CaCl_2$) could be achieved through the addition of extra $CaCl_2$. Based on this finding, a modified protocol was developed using 10−12 equiv of $CaCl_2$, and as such the

theoretical yield (based on solubility of **1c**) could be increased significantly (76−94% based on a total water charge of 30 L/kg input). For the heterogeneous protocol **1b** was suspended in water at a concentration of 10 L/kg input, and a solution of $CaCl_2$ (11 equiv) in water (10 L/kg) was added to the slurry. The mixture was stirred at 20 to 25 °C for 1 h, heated to 50 °C over 2 h to complete the salt exchange, and aged at 50 °C for 12 to 24 h. This protocol provided several advantages: the material was crystalline throughout the entire salt formation process with no gum or amorphous phase observed, as verified by optical microscopy, Figure 12; there was no requirement for dissolution of **1b** prior to the addition of $CaCl_2$; therefore, additional water could be used for the $CaCl_2$ charge (10 L/kg input) alleviating the abrupt supersaturation change that had been observed during the direct crystallization process. Seeding was not needed; however, it was employed to ensure polymorph control during the crystallization.

During this crystallization process the heterogeneous mixture goes through a very thick stage similar to that of the direct crystallization process due to the intrinsic fine-needle morphology of the crystals. The thickness of the slurry presents potential challenges for agitation, and insufficient agitation has been shown to lead to a stagnant mixing zone near the walls and bottom of the vessel. Over time the material in this stagnant zone can build into a shell or crust-like solid mass which hampers isolation. Another potential issue with crust formation is that the material may not mix with the bulk mixture and can lead to the presence of residual ammonium salt **1b** in the product. These problems were addressed by employing a two-stage water addition strategy, which involved a second water charge (6 L/kg input) after the slurry goes through its thickest stage. This allows any crust formed to be dislodged from the vessel walls into the bulk mixture as well as facilitating agitation by making the mixture less viscous. The additional water charge has an insignificant impact on yield since the solubility curve is essentially flat when using 3−5 wt % $CaCl_2$. During the transformation, Raman technology was employed to monitor the rate of formation of **1c** as well as to ensure complete conversion of **1b**. Compounds **1b** and **1c** have distinct peaks in the 980−1180 cm^{-1} and 1480−1550 cm^{-1} range that makes

Needles formed after 1 h @ rt   More needles observed after 2 h @ rt   Mostly needles observed after warming to 50 °C

Needles after 2 h @ 50 °C   Needles after 24 h @ 50 °C
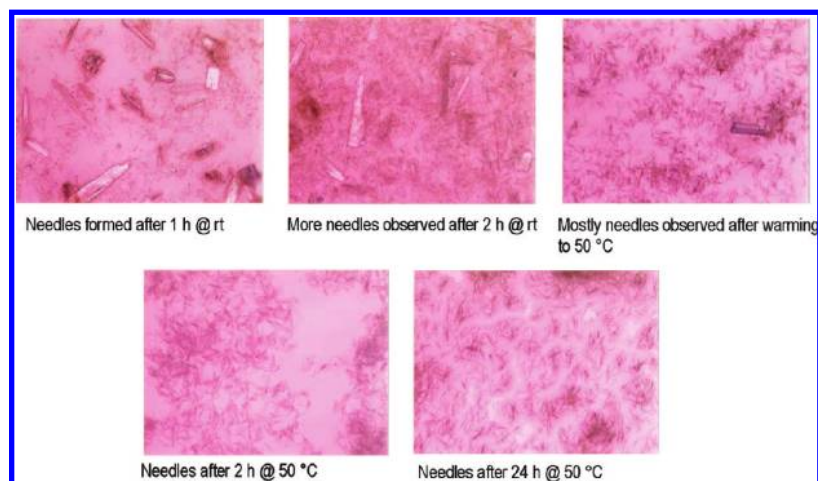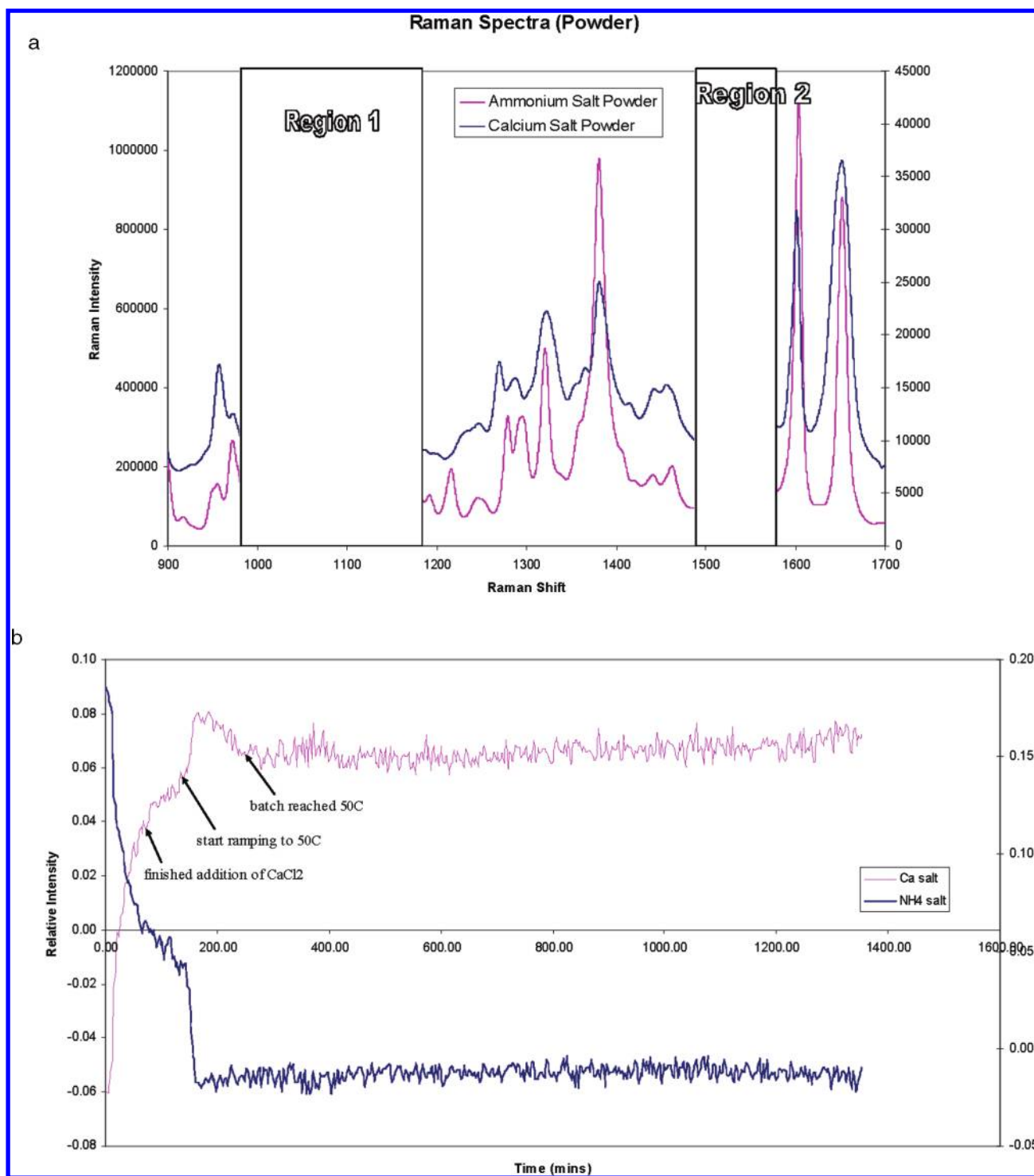
Figure 12. Evolution of crystals during the formation of **1c** via the heterogeneous crystallization protocol.

Figure 13. (a) Raman spectra for the conversion of 1b to 1c (b) Kinetic monitoring of the transformation of 1b to 1c by Raman technology.

Raman monitoring possible, Figure 13a. Figure 13b shows that the salt exchange from **1b** to **1c** starts at 20 to 25 °C and is completed once the batch temperature reaches 50 °C. The additional aging at 50 °C is employed to improve the particle

size of the product but is not a requirement for complete transformation.

Upon filtration, the cake was found to be highly compressible and retained mother liquor, thus making efficient deliquoring and washing difficult. After evaluating several filtration options, it was found that the use of a plate filter with a minimal head pressure together with charging the slurry in portions to build up the cake thickness was the preferred method for filtration. To displace the mother liquor retained in the cake, water and

(29) Roth, B. D. Preparation of *trans*-6-[(carbamoylpyrrolyl)alkyl]-4-hydroxypyranones as hypocholesterolemics. U.S. Patent 4,681,893, 1987.

(30) Hirai, K.; Ishiba, T.; Koike, H.; Watanabe, M. Pyrimidine derivatives as HMG-CoA reductase inhibitors. Eur. Pat. Appl. 1993, EP 521471, 1993.

heptane washes were incorporated, and the product was then dried in an agitated dryer until the KF was less than 10%. By utilizing the improvements described above the heterogeneous crystallization protocol was demonstrated on a 28 kg scale to provide the product in 80% yield with 99.3 area % and 82.8 wt % versus the free acid theoretical of 89.7 wt %.

Conclusion

In summary, this manuscript discloses the development of a robust, efficient and scalable synthesis of the HMGR inhibitor **1c**. Over the course of the development efforts numerous process improvements were achieved: chromatography was eliminated and replaced with selective and efficient crystallization protocols; safe and scalable syntheses of the aminotriazole and pyrimidine cores were developed and executed at scale. The development of the Julia−Kocienski olefination reaction led to the unprecedented dependence of product geometry on reaction temperature, such that an *E:Z* ratio in excess of 200:1 was obtained. The incorporation of an 'intermediate' salt drop was leveraged to ensure API quality prior to a heterogeneous salt-to-salt transformation. Key considerations in the development strategy and route selection included the careful evaluation of thermochemical safety and impurity control via the selection of process parameters, which was attained through the use of mechanistic first principles and process understanding. The result of these aspects culminated in the ability to prepare >70 kg of **1c** in 35% overall yield.

Experimental Section

The experimental outlined below provide representative procedures for what was run on scale in the kilo/pilot-plant facilities. Reagents and solvents were acquired from a variety of sources and employed without further purification. ^{1}H NMR spectra were obtained at 400 MHz, ^{13}C NMR spectra were obtained at 100 MHz and ^{19}F NMR spectra at 376.5 MHz at 25 °C in CDCl$_3$ except as indicated. Chemical shifts are reported in ppm downfield from an internal tetramethylsilane standard or relative to the residual solvent signal. Coupling constants (*J*) are given in hertz. Melting points were measured with a capillary melting point apparatus and are uncorrected. Moisture determinations were performed with a Karl Fischer titrator. HPLC analyses were performed using a reverse phase technique. Gas chromatographic analyses were performed with a J&W DB-1 column (30 m × 0.32 mm × 5 μm film thickness). A general GC method was employed: 1.6 mL/min flow rate (He carrier), FID, 1 μL injection volume, 250 °C injector port, running a gradient of 5 min at 50 °C, then to 225 °C at a rate of 20 °C/min, followed by a 10 min hold at 225 °C.

Methyl 4-(4-Fluorophenyl)-2-hydroxy-6-isopropylpyrimidine-5-carboxylate (12). A 20 L reactor was purged with nitrogen and charged with dihydropyrimidine **11** (700.0 g, 2.39 mol), CuCl$_2$ (3.25 g, 0.024 mol), K$_2$CO$_3$ (33.1 g, 0.243 mol), and CH$_2$Cl$_2$ (7.0 L). The starting material does not completely dissolve under these conditions. The suspension was heated to 35 °C and treated with *tert*-butyl hydroperoxide (70% aqueous solution) (635.0 g, 677.2 mL) over 120 min with vigorous agitation. After 24 h, HPLC indicated the consumption of the starting material (criterion:<1.0 area % of residual pyrimidine

11 by HPLC). The solution was cooled to 20−25 °C and treated with a mixture of aqueous Na$_2$S$_2$O$_3$ (0.5 M solution, 7.0 L) and 25 wt % aqueous NH$_4$Cl (3.5 L), and the resulting biphasic mixture was stirred vigorously for 60 min. The pH of the aqueous and organic phases should be ∼7.5−8.0. The two phases were separated, and the absence of remaining oxidant was checked using a peroxide test strip. If needed, an additional thiosulfate wash can be performed. The organic phase was concentrated to minimum volume via reduced pressure distillation. During the distillation, product **12** precipitated from the solution as a white solid. A solvent exchange to heptane was performed until the amount of residual CH$_2$Cl$_2$ was <10 vol % by GC. The product was filtered and washed with filtrate followed by heptane (1.0 L), and the wet cake was dried under vacuum (∼27 Torr) at 40 °C until an LOD of <1.0% was achieved. **12** was obtained in 95.8% isolated yield (666.1 g) as a white powder with HPLC purity of 99.6 area % and 97.6 wt %.

Methyl 4-(4-Fluorophenyl)-6-isopropyl-2-(1-methyl-1*H*-1,2,4-triazol-5-yl)amino)pyrimidine-5-carboxylate (14). A 400-L glass-lined reactor was purged with nitrogen and charged with dimethylformamide (93.5 kg), chloropyrimidine **10** (19.8 kg, 64.13 mol), and aminotriazole **7** (7.55 kg, 76.95 mol). The suspension was cooled to 0−5 °C, and potassium *tert*-butoxide (1.0 M solution in THF, 115.7 kg, 128.26 mol) was charged over 1 h, maintaining the batch temperature <15 °C. At the end of the potassium *tert*-butoxide addition, the reaction mixture temperature was raised to 18−25 °C, stirred for 1 h, and then sampled for HPLC analysis. HPLC typically indicated less than 0.5 area % of **10** remaining in the reaction mixture. If the amount of **10** remaining is ≥0.5%, an additional amount of base should be added. At this point the majority of the THF was removed by distillation at <40 °C under reduced pressure (100−130 Torr). The product was precipitated by the addition of water (198 kg) over 2 h while maintaining the temperature at 25−35 °C. During the water addition, the initial cloudy reaction mixture became clear and homogeneous. After ∼2/3 of the water has been added the product begins to crystallize. The slurry was stirred for >20 h at 20−25 °C and was then filtered. The wet cake was washed with a mixture of DMF/water (60 L 1:3 by volume) followed by 60 L of water. The wet cake was dried under vacuum at <50 °C. Compound **14** was obtained in 86% yield, ∼20.38 kg, with an HPLC purity of 99.9 area % and 99.4 wt %. ^{1}H NMR (400 MHz, CDCl$_3$): δ 1.21 (d, *J* = 6.59 Hz, 6H), 3.12 (m, 1H), 3.65 (s, 3H), 3.78 (s, 3H), 7.08 (dd, *J* = 8.33, 8.83 Hz, 2H), 7.55 (dd, *J* = 5.12, 8.66 Hz, 2H), 7.85 (s, 1H), 8.97 (s, 1H). ^{13}C NMR (100 MHz, CDCl$_3$): δ 22.3, 33.7, 36.7, 53.0, 115.6 (d, *J* = 21.7 Hz), 118.1, 129.9 (d, *J* = 8.3 Hz), 133.7 (d, *J* = 3.3 Hz), 148.2, 149.1, 159.2, 163.5 (d, *J* = 250.9 Hz), 163.8, 168.4, 175.0. ^{19}F NMR (282 MHz, CDCl$_3$): δ −112.1. ESIMS *m/z* 371 [M + H^{+}], mp 186.8 °C (dec). Anal. Calcd for C$_{18}$H$_{19}$FN$_6$O$_2$: C, 58.37; H, 5.17; N, 22.69. Found: C, 58.27; H, 4.90; N, 22.82.

(4-(4-Fluorophenyl)-6-isopropyl-2-(methyl(1-methyl-1*H*-1,2,4-triazol-5-yl)amino)pyrimidin-5-yl)methanol (16). A 1200-L Hastelloy reactor was purged with nitrogen and charged with dimethyl carbonate (104.7 kg), ester **14** (19.6 kg, 52.9 mol), and 1,4-diazabicyclo[2,2,2]octane (6.34 kg, 56.5 mol). The

suspension was heated to reflux (88−90 °C), stirred for 3−4 h, and then sampled for HPLC analysis. If the amount of residual starting material is >0.5 area %, the reaction mixture should be heated for another 2 h. Upon reaction completion, the reaction mixture was cooled to 20−25 °C, and water (20 L) and toluene (40 L) were charged. Any solids observed in the reaction mixture typically go into solution upon addition of the water. The phases were separated, and the upper organic phase was washed sequentially with 25 wt % aqueous phosphoric acid (52.2 kg), 5 wt % aqueous sodium bicarbonate solution (35 L), and saturated aqueous sodium chloride solution (52 L). The organic solution was concentrated to minimum volume via reduced pressure distillation, while maintaining the internal temperature at <50 °C. The solvent exchange to toluene was performed by repeated toluene addition (39.7 kg) and distillation until the amount of residual dimethyl carbonate and water were below <0.1 area % by GC and <500 ppm by KF, respectively. The concentrated mixture was diluted with toluene to a volume of ∼125 L and then cooled to −15 °C. To the reaction mixture was added DIBAl-H (74.7 kg, 1.5 M solution in toluene) over 2−3 h, maintaining the temperature below −5 °C. After the addition, the mixture was agitated for an additional 30 min at −15 to −5 °C and then sampled for HPLC analysis. If compound **15** is ≥0.5 area % HPLC, then additional DIBAl-H should be added (0.1 equiv portions). Upon completion the reaction was quenched by the addition of isopropanol (7.9 kg, 1 equiv per equiv of DIBAl-H added) to the solution, while maintaining the internal temperature <−5 °C. The addition was exothermic, and hydrogen gas was formed. The reaction mixture was heated to 20−25 °C and transferred into a solution of hydrochloric acid (132 L, 1 N) over 2−4 h, while maintaining the internal temperature between 15−20 °C. A precipitate formed during the quench which became a thick slurry. Toluene (113.0 kg) was charged, and the reaction mixture was heated to ∼30 °C and held with high agitation for 1 h. The phases were separated, and the organic phase was washed sequentially with water (65 L), 5 wt % aqueous sodium bicarbonate (65 L), and brine (77 L). All washes were performed at 30 °C. The organic solution was concentrated to ∼50 L via reduced pressure distillation, while maintaining the internal temperature <50 °C. During the distillation the product crystallized, and the suspension was stirred for 1 h at ∼40 °C prior to cooling to 20−25 °C. *n*-Heptane (33 L) was added over 1 h and the slurry stirred for an additional 2 h before cooling to 0−5 °C. The slurry was stirred at 0 °C for 2 h and then filtered. The wet cake was washed with a mixture of *n*-heptane/toluene (2:1, 22 L), followed by a wash with *n*-heptane (177 L). The wet cake was dried under vacuum at <50 °C until an LOD of <1.0% was achieved. The product **16** was obtained in 78% yield, 14.71 kg, with HPLC purity of 99.6 area % and 99.1 wt %. ^{1}H NMR (400 MHz, CDCl$_3$): δ 1.19 (d, J = 6.32 Hz, 6H), 2.20 (br s, 1H), 3.40 (m, 1H), 3.55 (s, 3H), 3.64 (s, 3H), 4.56 (br s, 2H), 7.10 (dd, J = 8.31, 8.79 Hz, 2H), 7.69 (dd, J = 5.38, 8.78 Hz, 2H), 7.82 (s, 1H). ^{13}C NMR (100 MHz, CDCl$_3$): δ 22.7, 31.9, 36.0, 37.2, 57.8, 115.1 (d, J = 21.6 Hz), 118.8, 131.0 (d, J = 8.5 Hz), 134.1, 149.2, 152.9, 159.3 163.1 (d, J = 247.5 Hz), 166.1, 177.3. ^{19}F NMR (282 MHz, CDCl$_3$): δ −112.0. ESIMS m/z 357 [M + H$^+$], mp 129.6 °C dec. Anal. Calcd for

C$_{18}$H$_{21}$FN$_6$O: C, 60.66; H, 5.93; N, 23.58. Found: C, 60.63; H, 5.88; N, 23.82.

4-(4-Fluorophenyl)-6-isopropyl-2-(methyl(1-methyl-1*H*-1,2,4-triazol-5-yl)amino)pyrimidine-5-carbaldehyde (9). To a 2000-L Hastelloy reactor, equipped with a 3-set pitch blade impeller and previously inerted with N$_2$, was charged **16** (29.63 kg, 83.12 mol, 98.75 wt %), TEMPO (1.30 kg, 8.32 mol), and KBr (500 g, 4.20 mol) as solids. This was followed by the addition of EtOAc (270.6 kg) and H$_2$O (78.28 kg). The batch was agitated at 80 rpm, and a recirculation loop with in-line Raman and pH probes was started. The batch was cooled to between 0 and −5 °C, and a titrated/nonbuffered sodium hypochlorite (NaOCl) solution (64.03 kg, 10.96 wt %) was added slowly over ∼2 h, at such a rate that the internal temperature of the batch did not exceed 5 °C. Upon complete addition, the batch temperature was maintained between −5 and 5 °C for 20 min before sampling the biphasic mixture for reaction completion. Upon reaching the in-process control criterion of <0.5 area % of **16** by HPLC, a 1.0 M sodium thiosulfate solution (173.4 kg) was prepared and charged over ∼20 min in order to quench the reaction mixture. The batch was warmed to 20−25 °C, stirred for ∼15 min, and analyzed for residual oxidant using a potassium iodide−starch test. Upon obtaining a negative test result, the agitation was ceased, and the biphasic mixture was allowed to settle for 10 min. The phases were separated, and the organic-rich layer was treated with a 0.5 M sodium hydroxide solution (240.5 kg). After agitating the biphasic mixture at 25 °C for 15 min, the layers were separated, and the organic layer was checked by HPLC analysis for the presence of acid impurity **17** (criterion <1.0 area %). The organic phase was washed with H$_2$O (300.4 kg). Following separation of the layers the organic layer was transferred to a clean reactor followed by an ethyl acetate rinse (30.2 kg). The organic layer was concentrated via distillation to a target volume of 60 L (T_{batch} = 62 °C; vac = 300−400 mmHg; T_{jacket} = 83 °C). Isopropyl alcohol (141.3 kg) was charged in portions (5−10 kg at a time in order to maintain a level of 60−90 L in the tank, semibatch mode), and the distillation/solvent swap was continued until a final target volume of 60 L (T_{batch} = 62−65 °C; vac = 350−400 mmHg; T_{jacket} = 83 °C) was reached. An additional charge of isopropyl alcohol (23.8 kg) was added, and the sample was assayed for residual EtOAc (criterion: <1 vol %). Water (70.0 kg) was added, maintaining the batch temperature between 60−65 °C in order to reach 30 vol % of water in IPA; a slurry was observed prior to the completion of the H$_2$O charge. The resulting thick slurry was cooled to 10 °C over 2 h and held overnight. The slurry was filtered in two loads on a centrifuge, and each load was washed with 1:3 IPA/H$_2$O (56.8 kg) and H$_2$O (41.1 kg). The resulting white crystalline solid was dried at ∼25 °C, under full vacuum until the KF was <0.5%, furnishing 27.64 kg of **9** in 93.5% yield with 99.88 area % and 99.63 wt %.

tert-**Butyl 2-((4*R*,6*S*)-6-((*E*)-2-(4-(4-fluorophenyl)-6-isopropyl-2-(methyl(1-methyl-1*H*-1,2,4-triazol-5-yl)amino)pyrimidin-5-yl)vinyl)-2,2-dimethyl-1,3-dioxan-4-yl)acetate (8b).** To a 600-L cryogenic reactor was charged compound **9** (27.5 kg, 77.6 mol), compound **5** (38.4 kg, 84.86 mol), and THF

(244.5 kg). The batch was stirred for 15 min to ensure dissolution of the solids. The solution was cooled to −80 °C and LiHMDS (63.7 kg, 1.2 equiv) was charged over 80 min keeping the batch temperature below −70 °C throughout. After a further 5 min HPLC analysis indicated 1.2 area % of compound **9** remaining (criterion: 2 area %). The batch was warmed to −10 °C, and after 1 h an *E:Z* product ratio of 91:1 was observed. The reaction was quenched with a 10% aqueous potassium bicarbonate solution (137.5 kg), and the batch was warmed to 15−25 °C. After agitating for 5 min and settling for 15 min the aqueous phase was drained and a second portion of 10% aqueous potassium bicarbonate (137.5 kg) was charged. The mixture was agitated for 5 min and allowed to settle for 1 h to provide a clean phase split. Ethanol SDA3A (173.5 kg) was added, and the solution was transferred to a 1900-L reactor through a 10 μm polish filter. Additional ethanol SDA3A (174.6 kg) was introduced and the solution concentrated by vacuum distillation (150 mmHg) from 766 to 270 L. Ethanol SDA3A (195.3 kg) was charged at which point analysis by GC showed 4.4 vol % of THF remaining (criterion: 6 vol %). Water (330.0 kg) was added over 5 h, keeping the batch temperature at 38−42 °C, and the resulting slurry was held at this temperature for 2 h. The batch was cooled to 18−20 °C over 90 min and held for 1 h, at which point analysis showed 0.19 wt % product in the mother liquor. The slurry was filtered, and the cake was washed with 60% ethanol SDA3A in water (300 kg). The wet cake was dried without agitation under full vacuum for 32 h (LOD = 0.9%) followed by drying with periodic agitation for 24 h (final LOD = 0.5%). The final product **8b** was isolated as a white solid, 33.58 kg with 99.92 area % and 99.2 wt % (74.2% adjusted yield).

Ammonium (3*R*,5*S*,*E*)-7-(4-(4-Fluorophenyl)-6-isopropyl-2-(methyl(1-methyl-1*H*-1,2,4-triazol-5-yl)amino)pyrimidin-5-yl)-3,5-dihydroxyhept-6-enoate Monohydrate (1b). Compound **8b** (35.00 kg, 60.27 mol) was charged to a 1900-L reactor, followed by acetonitrile (275 kg). To the resultant slurry was added hydrochloric acid (0.02 N, 151.20 kg, 3.01 mol) at 20−25 °C, and an endotherm to 10 °C occurred. The slurry was heated to 40−45 °C for 3 h until the area % of compound **8b** remaining was <2 area %. The resultant solution was cooled to 20−25 °C, and NaOH (2 N, 43.75 kg, 90.41 mol) was added. The solution was stirred at 20−25 °C for 1 h until compound **19** had <1 area % remaining. Water (WPUR) (175.0 kg) was charged to the reactor followed by heptanes (145.1 kg). The mixture was agitated at 20−25 °C for ∼10 min. Agitation was stopped, and the two phases were allowed to separate, ∼15 min. The two phases were separated, and the product-rich aqueous layer was recharged to the reactor. To this aqueous solution was added hydrochloric acid (1 N) until the pH reached between 7 and 8, (amount of 1 N HCl required was 29.5 kg). Isopropyl acetate (252.0 kg) was added, and the pH continued to be adjusted with hydrochloric acid (1 N) until the pH was between 2.2 and 2.8, (amount of 1 N hydrochloric acid added was 59.9 kg). Agitation was continued for 10 min. The two phases were allowed to separate. The organic layer was washed with a 10 wt % brine solution (192.5 kg). After agitating for 10 min the two phases were allowed to separate. The phases were separated, and the organic phase was transferred to a clean reactor through

a 0.5 μm polish filter. The temperature of the batch was set to 20−25 °C. Ammonia gas (0.12 kg, 6.63 mol) was added to the solution over ∼30 min. The batch was seeded with a slurry of compound **1b** (35 g) in isopropyl acetate (274 g) and held for 5 min at 20−25 °C. The remaining ammonia gas (1.01 kg, 59.67 mol) was added over a period of at least 2 h. A sample of the slurry was taken to ensure that the pH was >8 by pH paper, and the slurry was held at 20−25 °C for 15 h. A sample was removed to ensure the liquor concentration was <0.5 wt % of compound **1b**. On meeting this criterion the batch was filtered, and the cake was washed in portions with isopropyl acetate (122.0 kg). The cake was dried at <40 °C under vacuum until the wt % of isopropyl acetate was less than 0.2 wt %. **1b** was isolated as a white powder, 27.61 kg (89.5% yield, 99.85 wt %, 99.4 area %).

Hemi-calcium (3*R*,5*S*,*E*)-7-(4-(4-Fluorophenyl)-6-isopropyl-2-(methyl(1-methyl-1*H*-1,2,4-triazol-5-yl)amino)pyrimidin-5-yl)-3,5-dihydroxyhept-6-enoate Dehydrate (1c). Compound **1b** (ammonium salt) (28.4 kg) was charged to an inerted 1900 L Hastelloy reactor. Water (284 kg, 10 L/kg input) was added to produce an aqueous slurry of **1b** which was held at 20 °C. In a separate Hastelloy vessel, anhydrous $CaCl_2$ (44.6 kg, 11 equiv) was dissolved in water (284 kg 10 L/kg input). The aqueous $CaCl_2$ solution (13.6 wt %) was transferred into the reactor containing the slurry of **1b** using pressure via a CUNO filter. Following the addition of the $CaCl_2$ solution, the slurry was held at 20 °C for ∼60 min. Heat was then applied to the reactor jacket to heat the slurry to 50 °C over a 2 h period. When the temperature reached ∼31 °C, the slurry was observed to thicken, and the agitation was increased to maintain good mixing. When the batch reached 50 °C, water (170.4 kg, 6 L/kg input) was charged to the slurry, and the slurry was then aged at 50 °C for 14 h. After aging, the batch was cooled to 20 °C. The batch had a total volume of ∼800 L and was filtered in three portions on a 36-in. Nutsche plate filter. Each load was washed three times with water (79 kg) followed by a heptane displacement wash (109 kg). The combined wet cake was then dried in a 500 L conical dryer at 50 °C with full vacuum and intermittent agitation until the KF was <10 %. The product **1c** was obtained as an off-white powder, 23.88 kg, in 79.9% yield with 99.3 area % and 82.8 wt %.